

Original Article

Cite this article: Moreau J-D, Trincal V, Deconinck J-F, Philippe M, and Bourel B (2021) Lowermost Jurassic dinosaur ecosystem from the Bleymard Strait (southern France): sedimentology, mineralogy, palaeobotany and palaeoichnology of the Dolomitic Formation. *Geological Magazine* **158**: 1830–1846. <https://doi.org/10.1017/S001675682100039X>

Received: 30 October 2020

Revised: 3 April 2021

Accepted: 15 April 2021

First published online: 17 May 2021


Keywords:

conifers; Cheirolepidiaceae; theropod footprints; paralic palaeoenvironments; Hettangian; Lozère

Author for correspondence: Jean-David

Moreau, Email: jean.david.moreau@gmail.com

Lowermost Jurassic dinosaur ecosystem from the Bleymard Strait (southern France): sedimentology, mineralogy, palaeobotany and palaeoichnology of the Dolomitic Formation

Jean-David Moreau¹ , Vincent Trincal², Jean-François Deconinck¹, Marc Philippe³ and Benjamin Bourel⁴

¹CNRS UMR 6282 Biogéosciences, Université de Bourgogne Franche-Comté, 6 boulevard Gabriel, 21000 Dijon, France; ²LMDC, INSAT/UPS Génie Civil, 135 Avenue de Rangueil, 31077 Toulouse cedex 04, France; ³Université de Lyon, Claude-Bernard Lyon-1, ENTPE, CNRS, UMR 5023 LEHNA, 69622 Villeurbanne, France and ⁴Aix Marseille Univ, CNRS, IRD, INRA, Coll France, CEREGE, 13545 Aix-en-Provence, France

Abstract

We report the first Hettangian theropod tracksite (~200 Ma) yielding a rich accumulation of plant remains from the Bleymard Strait (southern France). It constitutes an excellent opportunity to reconstruct lowermost Jurassic ecosystems hosting dinosaurs and which are still poorly documented in this area. Two morphotypes of tridactyl tracks are distinguished. They share similarities with *Grallator* and *Kayentapus*. Plant-bearing beds yield abundant leafy axes (*Pagiophyllum peregrinum*), male cones (*Classostrobus* sp.), wood (*Brachyoxylon* sp.) and pollen of conifers (*Classopollis classoides*). Sedimentological, petrological and mineralogical analyses demonstrated that, in the Dolomitic Formation from Bleymard, the palaeoenvironment progressively evolved from (1) a shoreface to a foreshore domain; to (2) a shallow environment that is restricted or occasionally open to the sea; then to (3) an intertidal to supratidal zone. The Hettangian theropod ecosystem of the Bleymard Strait was composed of tidal flats that were periodically emerged and bordered paralic environments inhabited by a littoral conifer-dominated forest in which Cheirolepidiaceae were the main component. The paucity of the palaeobotanical assemblage, as well as the xerophytic characteristics of *Pagiophyllum*, show that flora from Bleymard was adapted to withstand intense sunlight and coastal environments exposed to desiccant conditions coupled with salty sea spray, and dry conditions. These features are those of a conifer-dominated flora under a tropical to subtropical climate. The flora as well as the clay mineral analyses suggest contrasting seasons (cyclically dry then humid). This study supports that theropods were abundant and particularly adapted to this type of littoral environment bordering Cheirolepidiaceae-dominated forests.

1. Introduction

The Hettangian was a crucial period in the evolution of Dinosauria, corresponding to the end of the Late Triassic – Early Jurassic evolutionary radiation of the clade (Brusatte *et al.* 2008). However, Hettangian-aged geological units showing a co-occurrence of dinosaur remains (e.g. Larsonneur & Lapparent, 1966; Delsate & Ezcurra, 2014) and associated faunas or floras are rare in Europe. In this context, deposits containing dinosaur tracks and associated fossils constitute an excellent opportunity to reconstruct lowermost Jurassic ecosystems hosting dinosaurs and which are still poorly documented.

The Causses Basin in southern France is known for its abundant Jurassic archosaur footprints (Demathieu *et al.* 2002; Gand *et al.* 2007). The Hettangian Dolomitic Formation from this area yielded abundant vertebrate tracks mainly ascribed to theropod dinosaurs and more rarely to crocodylomorphs (Ellenberger, 1988; Demathieu, 1990; Demathieu & Sciau, 1992, 1999; Demathieu *et al.* 2002; Sciau, 2003; Moreau *et al.* 2012a, 2014, 2019a). Dozens of tracksites were reported from the French departments of Aveyron, Gard and Lozère. However, because fossils are extremely rare in the Dolomitic Formation, our knowledge of Early Jurassic ecosystems inhabited by dinosaur communities is limited in this area.

A new palaeontological site showing the co-occurrence of rich plant-bearing beds and dinosaur tracks was discovered from the Dolomitic Formation of the Bleymard Strait (Lozère). Although palaeofloras were previously reported from Hettangian–Sinemurian deposits of several localities in the Causses Basin (e.g. Saporta, 1873, 1884; Ressouche, 1910; Roquefort, 1934; Barale *et al.* 1991; Thévenard, 1992, 1993; Moreau & Thévenard, 2018; Moreau *et al.* 2019b), they were rarely reported and undescribed associated with dinosaur tracksites (Sciau, 1992).

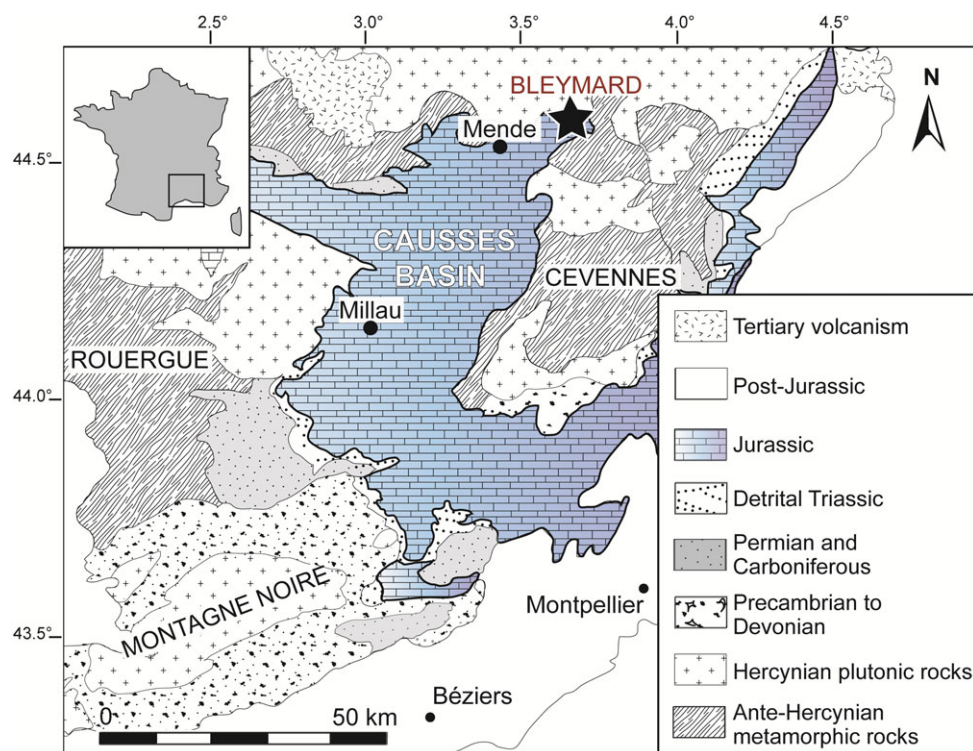


Fig. 1. (Colour online) Location and geological context of the Causses Basin with the geographical position of the Bleymard Strait.

The discovery presented here consists of the first Hettangian dinosaur tracksite yielding plant-rich beds in the Bleymard Strait.

The main objective of this research was to reconstruct Hettangian dinosaur ecosystems from Bleymard using a multi-proxy approach. Sedimentology, petrology and mineralogy analyses are combined to characterize the lithofacies and to understand the evolution of the depositional environments. Palaeoichnological analyses based on vertebrate tracks and palaeobotanical analyses based on cuticles, wood and pollen are used to reconstruct the ichnofaunas and palaeofloras.

2. Geographical and geological setting

The fossil plants and dinosaur tracks described here have been discovered in a small quarry in the Bleymard Strait area, in the northeastern extremity of the Causses Basin (Occitanie, southern France). The quarry is located in the Lozère department, 25 km to the east of Mende (Fig. 1). In the Causses Basin, Hettangian deposits are divided into two formations: the Detrital Sandstones – Variegated Mudstones Formation and the Dolomitic Formation (Brouder *et al.* 1977; Briand *et al.* 1979; Gèze *et al.* 1980).

The Detrital Sandstones – Variegated Mudstones Formation consists of rubefied lenticular and channelized sandstones that alternate with variegated argillite or marl (Simon-Coinçon, 1989). Near Bleymard, the Detrital Sandstones – Variegated Mudstones Formation is poorly developed (c. 0–30 m thick; Briand *et al.* 1993) and is largely dominated by sandstone and conglomerate. According to Briand *et al.* (1993), this formation does not yield any fossils near Bleymard. However, the Detrital Sandstones – Variegated Mudstones Formation yields rare plant impressions (e.g. Malafosse, 1873; Saporta, 1891; Moreau & Thévenard, 2018) as well as dinosaur tracks (Moreau *et al.* 2012b) in the northern part of the Causses Basin. Plant remains consist of Bennettitalean vegetative structures ascribed to

Otozamites latior Saporta and Bennettitalean fructification such as *Weltrichia fabrei* Saporta emend. Moreau & Thévenard (Saporta, 1891; Moreau & Thévenard, 2018).

Near Bleymard, the lower part of the Dolomitic Formation consists of dolomite as well as sublithographic limestone organized in massive layers (0–20 m thick), whereas the upper part of the formation consists of thin layers of yellow-coloured limestone alternating with green to blue argillite (20–40 m thick; Briand *et al.* 1993). The fossiliferous beds exposed in the Bleymard quarry are located in the lower part of the Dolomitic Formation. The rare ammonites (e.g. *Psiloceras planorbis* Sowerby; Brouder *et al.* 1977) which were described from the Dolomitic Formation of Lozère confirm the Hettangian age of this formation.

3. Material and methods

3.a. Sedimentology and mineralogy

Detailed sedimentological, petrographic and mineralogical analyses were conducted along a 13 m thick stratigraphic section that could be accessed in the Bleymard quarry (Fig. 2). Fourteen lithostratigraphic levels were distinguished (Fig. 2). Each of them was sampled (BL.S1–BL.S14) in order to both conduct optical microscopy on standard polished thin-sections and to perform mineralogical analyses on ground samples. Based on field observations as well as microfacies and mineralogical analyses, we have characterized the evolution of the depositional environments along the section. X-ray fluorescence spectrometry (XRF) and X-ray diffraction (XRD) measurements were performed at the Civil and Environmental Engineering Department, LGCgE of IMT Lille–Douai, following the methods described in Moreau *et al.* (2018) and Trincal *et al.* (2018).

XRF analyses were performed using a Bruker S4 Pioneer spectrometer and a 4 kW wavelength dispersive X-ray fluorescence spectrometer equipped with a rhodium anode. Measurements were

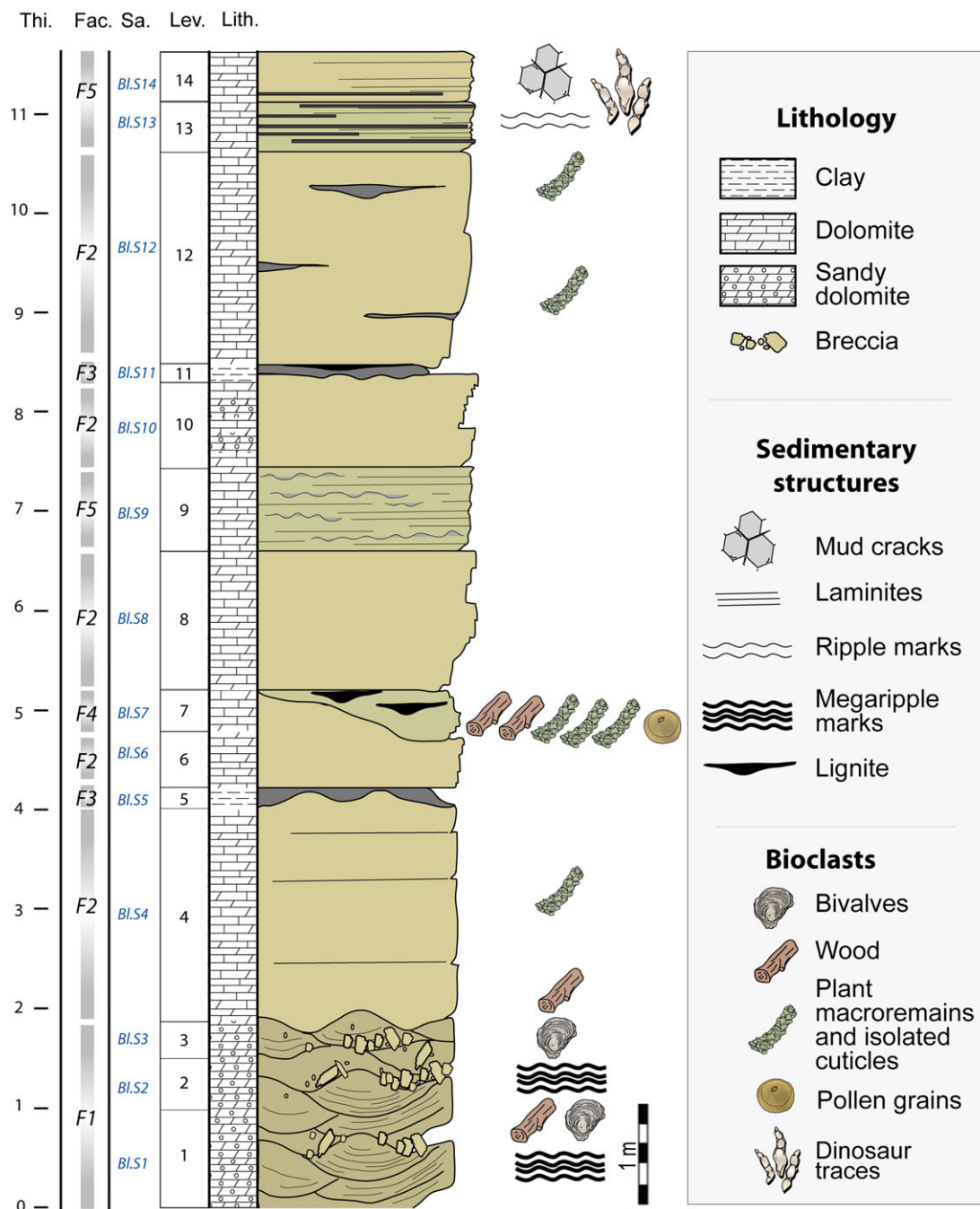


Fig. 2. (Colour online) Stratigraphic section of the Bleynard quarry showing the location of the dinosaur tracks and plant remains. Thi., thickness (m); Fac., facies; Sa., location of samples taken; Lev., levels; Lith., lithology.

taken at 60 keV and 40 mA on powdered rock-compressed tablets. XRD diffractograms were obtained with a Bruker D8 Advance diffractometer system using Co-K α radiation equipped with a fast LynxEye position sensitive detector (WL = 1.74). The diffractometer was operated at 35 kV and 40 mA. Scans were run from 5° to 60–80°2 θ , with a step interval of 0.02°2 θ and a time acquisition of 96–192 s per step. Two protocols were used: the first to quantify the bulk rock minerals; the second for the clay fraction (particles < 2 μ m) only.

Bulk rock minerals were identified from powders (thoroughly dried and micronized by grinding with an agate mortar and pestle) using the Bruker-AXS DiffracPlus EVA software and the

International Centre for Diffraction Data (ICDD) Powder Diffraction File 2015 database. Quantification was achieved using the Rietveld method (e.g. Rietveld, 1969; Snyder & Bish, 1989; Bish & Post, 1993) with the DIFFRACplus TOPAS software, version 4.2 (Bruker-AXS), and the crystal structure data were taken from the ICDD PDF and Bruker Structure Database. For more information about the Rietveld method and estimates of accuracy, refer to Taylor & Hinczak (2006) and Trincal *et al.* (2014).

Clay mineral extraction was carried out by sedimentation after a treatment with a weak-concentration hydrochloric acid. At least three XRD runs were performed on the oriented mounts following air-drying, ethylene-glycol solvation and heating at 550 °C for 2 h

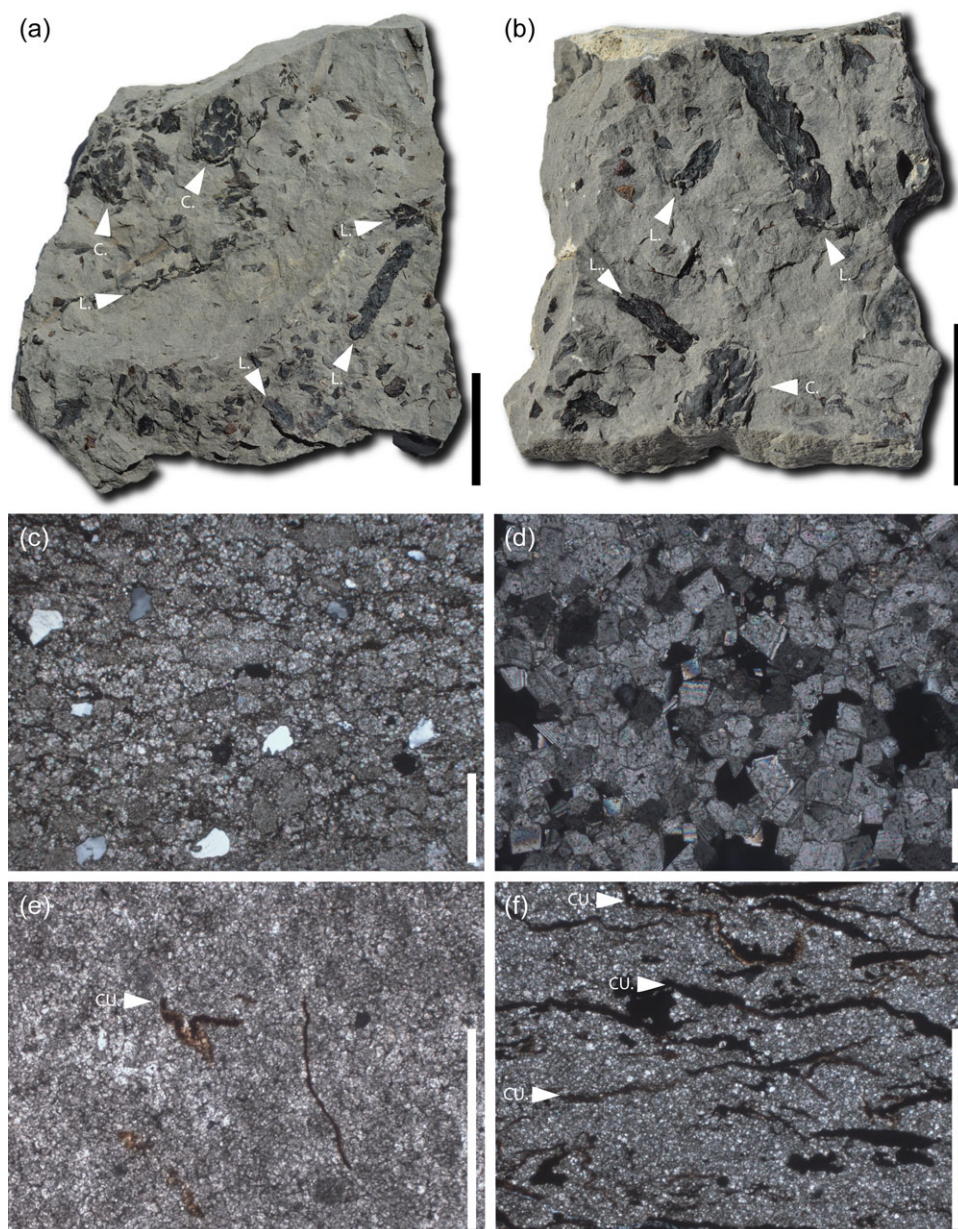


Fig. 3. (Colour online) Facies and microfacies. (a–b) Dolomitic slabs from the main fossiliferous bed (facies F4) showing accumulations of conifer remains preserved as compressed cuticles; C., cones; L., leafy axes; specimens, (a) M486_2020.4_9, (b) M486_2020.4_1. (c–d) Sandy dolomite showing quartz grains (c) and dolomite crystals (d) (facies F1). (e) Dolomudstone showing some plant cuticles (facies F2). (f) Plant-bearing dolomite showing abundant plant cuticles (facies F4). Scale bars: (a–b) = 20 mm; (c, e–f) = 1 mm; (d) = 100 μm.

(Moore & Reynolds, 1997; Thiry *et al.* 2013). Clay minerals were identified according to the position of the (001) series of basal reflections on the three XRD diagrams; qualitative quantification using the RIR method (e.g. Klug & Alexander, 1974; Hillier, 2000, 2003; Trincal *et al.* 2018). The intensity peaks of the illite 001 (10 Å) and kaolinite 001 (7 Å) were used with RIR ratios of 1 and 2.4, respectively (Hillier, 2003). The relative content between kaolinite and chlorite was evaluated using the intensities of the 002 peak (3.58 Å) for kaolinite and the 004 peak (3.54 Å) for chlorite (Biscaye, 1964).

3.b. Palaeobotany

Plant beds in the Bleynard quarry were first observed by one of us (J.-D.M.) in 2009. Four levels yielded plant meso-remains: levels 1, 4, 7 and 12 (Fig. 2). In levels 1, 4 and 12, plants are rare

and mainly preserved as tiny impressions (i.e. external casts < 1 cm) of wood fragments or isolated cuticles. However, level 7 yields abundant compressions preserving cuticles (Fig. 3a–b), and most of the specimens studied here were collected from this level. Plant remains vary greatly in size and consist of micro- to macro-remains. Wood remains consist of millimetric to pluricentimetric fragments. The collection includes hundreds of well-preserved specimens, and these consist of leafy axes, isolated leaves, cones, wood and pollen grains of conifers. Specimens are housed in the collections of the Musée du Gévaudan (Mende, Lozère, France).

Cuticle analysis. Sediment was soaked in a solution of hydrogen peroxide (12 %) and water for a few days. The disaggregated sediment was then washed with tap water through a column of sieves (1.0 mm and 0.5 mm meshes). Fossils were picked out by naked eye or under a stereomicroscope. SEM micrographs were taken using a

Hitachi TM-1000 scanning electron microscope at Biogéosciences, Univ. Bourgogne Franche-Comté (Dijon) and a JEOL JSM5600 scanning electron microscope in Femto laboratory, Univ. Bourgogne Franche-Comté (Besançon).

Wood analysis. Wood samples superficially look like fusain, as they are black, brittle and glossy. Microscopic examination, however, revealed that tracheid walls retained fibrous structure. The fossil wood is rather an evolved lignite, which was investigated by pyroxylin microcasting. Parlodion was dissolved in amylacetate to a thick paste-like consistency, and applied in a 1 mm-thick layer on an area selected under the microscope as featuring a well-preserved radial breaking plan. This was allowed to dry for 24 hours and then carefully lifted. This translucent peel was mounted on glass and examined under a microscope. This inexpensive, quick and easy method is not suitable for the preparation of photographs, as the peel surface is too irregular, but it is efficient for the observation of the characteristic wood features.

Pollen analysis. We used the following standard procedure: (1) immersion of 2 g of sediment in HCl (33 %, 1 h) to remove the carbonates; (2) digestion in HF (48 %, 12 h); (3) immersion in HCl (33 %, 4 h) to remove the fluorosilicates produced in the previous step; and (4) immersion in KOH (20 %, 10 h) in a heated bath to remove the organic matter. Next, the sample was sieved at 150 µm, and then we used heavy liquid (sodium polytungstate) at a specific gravity 2.2 kg m⁻³ to separate the pollen in the <150 µm fraction.

3.c. Ichnology

A single bed (level 14) yields tridactyl dinosaur tracks (Fig. 2). The track-bearing surface was discovered in 2015. The descriptive terminology and biometric parameters used are derived from Leonardi (1987) and Marty (2008). We used the following standard abbreviations: length of the trace, 'L'; width of the trace, 'W'; and divarication angle between digit II and digit IV, 'II–IV'.

4. Results

4.a. Stratigraphy, petrography and mineralogy

Sedimentological, petrographic and mineralogical analyses distinguish five lithofacies, F1 to F5 (Table 1). The base of the stratigraphic section (from 0 to 2 m) displays plurimetric dunes showing large megaripple marks and oblique stratification (Fig. 2). These dunes correspond to F1 which consists of yellow to grey mudstone–packstone sandy dolomite locally yielding breccia and coquina lenses (Fig. 3c–d; Table 1). F1 is mainly composed of dolomite (weight percentage of 90 to 97 wt %) and quartz (1.5 to 6 wt %), with traces of clay confirmed by the presence of Al and Fe using XRF. Almost 80 wt % of illite and 20 wt % of kaolinite were identified among these clays (Figs 4–5; Fig. S1 and Tables S1–S3 in the Supplementary Material available online at <https://doi.org/10.1017/S001675682100039X>). Kaolinite peaks are very narrow, indicating that this mineral is very well crystallized. Quartz is also present in the clay fraction with an unusual high-intensity ratio between the (100) peak at 4.26 Å and the (101) peak at 3.33 Å.

F2 corresponds to a brown to grey dolomudstone organized in planar pluridecimeteric to metric beds (Fig. 2). F2 yields some tiny impressions (i.e. external casts) and cuticles of foliar plant remains, as well as wood fragments (Fig. 3e; Table 1). This facies is mainly composed of carbonates (85 to 98 wt % of dolomite and 0 to 10 wt % of calcite), as well as quartz and clay (mainly represented by illite) to a lesser extent (sum up to 5 wt %; Figs 4–5; S1–S3 in

the Supplementary Material available online at <https://doi.org/10.1017/S001675682100039X>).

F3 consists of green-blue to black clay (mudstone) organized in up to 20 cm thick lenses and which is locally lignitic (Table 1). This facies displays a high content of clay (more than 72 wt %) and quartz (almost 17 wt %; Figs 3–4; Tables S1–S3 in the Supplementary Material available online at <https://doi.org/10.1017/S001675682100039X>). Compared with other facies, carbonates are scarce (less than 9 wt %) whereas titanium oxide is particularly abundant (almost 2 wt %; Supplementary Table S2). In all of the other facies, rutile is almost absent, as confirmed by XRF analyses where titanium is detected in trace amounts (i.e. ≤0.1%; Supplementary Table S1). The clay fraction is essentially composed of poorly crystallized illite showing a high 001/002 ratio suggesting an iron-rich composition of this mineral (Figs 4–5; Supplementary Fig. S1; Supplementary Tables S1–S3).

F4 is characterized by grey to blue, clayey dolomite (mudstone–packstone texture) showing lenticular, and dark, thin (millimetric to centimetric) lignitic layers bearing abundant plant micro- to macro-remains (Fig. 3a–b, f; Table 1). F4 characterizes the main fossiliferous bed (level 7) which is a 50 cm thick lens that pinches out laterally. Chemically and mineralogically, F4 is close to F1, but shows a little more clay which this time is more concentrated in the illite (Figs 4–5; Tables S1–S3 in the Supplementary Material available online at <https://doi.org/10.1017/S001675682100039X>).

Finally, F5 consists of grey-blue to yellow dolomite locally organized in millimetric laminites in the transverse section (Table 1). Bedding plane surfaces of laminites bear mud cracks. The microbial laminae are parallel to the bedding planes and are wavy to planar. They show alternating dark microbial laminae and more transparent laminae composed of dolomitic mudstone. The cryptalgal laminites mainly exhibit a porous fabric with bioturbations. At the top of the stratigraphic section, F5 bears dinosaur footprints (level 14). Microfossils are absent from F5. The chemistry and mineralogy of F5 display a strong similarity with F1 and F4 which consist of almost 90 wt % Mg-rich carbonates and 10 wt % silicates and phyllosilicates. Unlike all of the other facies containing kaolinite and sometimes chlorite, only illite was observed in the F5 decarbonated clay fraction (Figs 4–5; Tables S1–S3 in the Supplementary Material available online at <https://doi.org/10.1017/S001675682100039X>).

4.b. Systematic palaeontology

4.b.1. Plants

Order – Coniferales

Family – Cheirolepidiaceae

Leafy axes

Pagiophyllum peregrinum (Lindley & Hutton) A. Schenk emend. Kendall

Material. M486_2020.4_1a; M486_2020.4_2 to M486_2020.4_8; M486_2020.4_13 to M486_2020.4_17.

Description. The leafy axes are up to twice branched and straight to slightly curved (Fig. 6). The longest specimen is 12 cm long. The shoots are narrow and up to 7 mm in diameter. The leaves are persistent, helically arranged (phyllotaxy 2/5 and 3/8), appressed and imbricated (Fig. 6). The leaves are scale-like, triangular to rhomboidal, 'longer than wide' up to 'as long as wide', and keeled on the abaxial side (Figs 6–7). They are 2.0–4.1 mm long, 1.6–2.9 mm wide (based on 13 measured specimens). Apically, the leaves display a short free part which is 0.3–1.2 mm long. The abaxial surface of leaves is convex, whereas the adaxial surface

Table 1. Microfacies. M, mudstone; W, wackestone; P, packstone; G, grainstone.

No.	Facies	Texture	Description	Depositional environments
F1	Sandy dolomite	(M)-W-P	Grey-brown to yellow mudstone–packstone sandy dolomite with oblique stratifications, locally showing breccia and coquina lenses. Some tiny wood fragments.	Shoreface to foreshore. High hydrodynamism.
F2	Dolomudstone	M (G)	Grey-brown dolomudstone locally yielding cuticles and external casts of plant meso-remains. Characteristic conchoidal fracture. Rare lenses of sandy dolomite.	Shallow environment not, or only partially/occasionally, open to the sea.
F3	Clay	M	Green-blue to black clay which is locally lignitic.	
F4	Plant-bearing dolomite	M-P	Grey-blue, clayey dolomite (mudstone–packstone texture) showing lenticular and dark thin (millimetric to centimetric) lignitic layers bearing abundant plant micro- and meso-remains (isolated leafy axes, leaves, cones and pollen of conifers as well as compressed woods).	
F5	Laminated dolomite	M	Grey-blue to yellow dolomite locally cryptalgal and showing abundant thin laminites in transverse section. The surfaces of the laminites bear mud cracks. The microbial laminae are parallel to the bedding planes and wavy to planar. They show alternating dark microbial laminae and more transparent laminae composed of dolomitic mudstone. The cryptalgal laminites mainly exhibit highly bioturbated porous fabric and a mudstone texture. Presence of dinosaur tracks.	Intertidal to supratidal zone. Tidal flat. Periodic emersions.

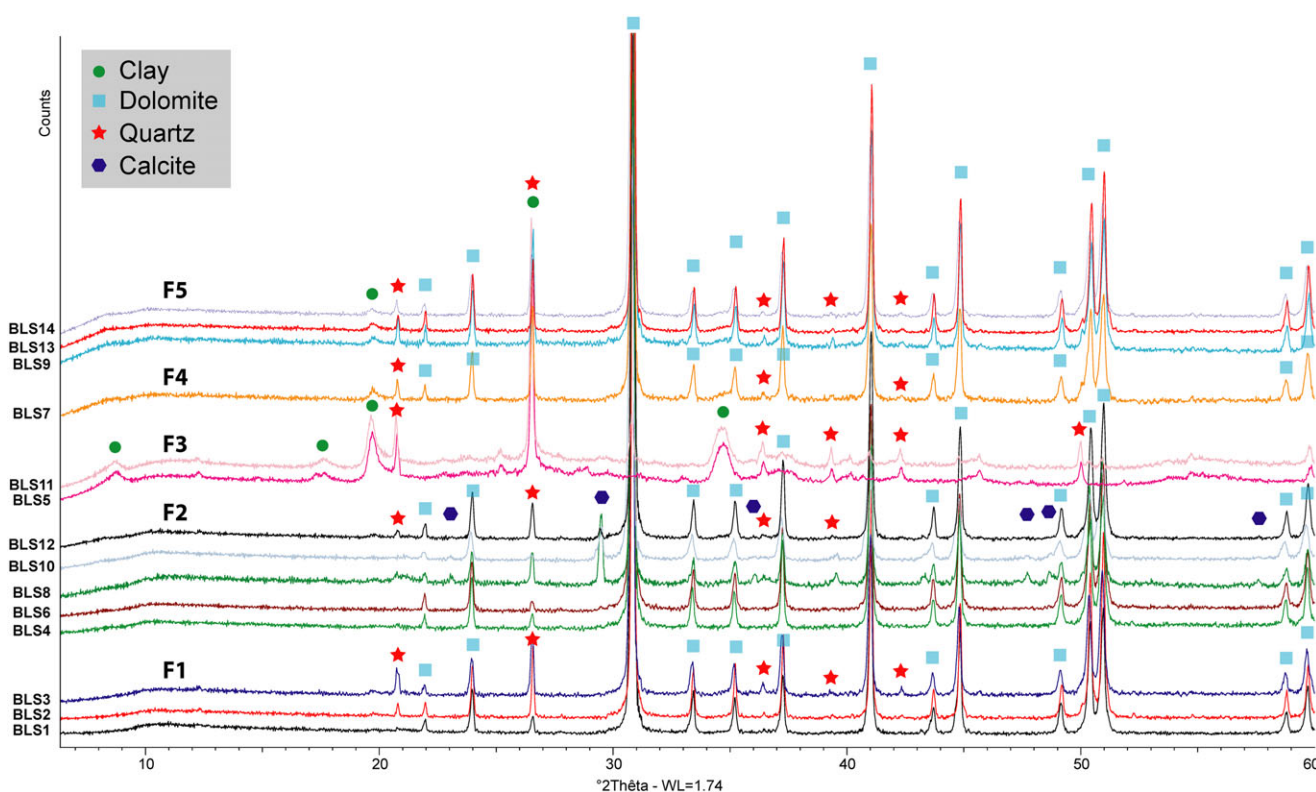


Fig. 4. (Colour online) Bulk rock XRD analyses of the Bleynard samples. The stratigraphic locations of samples BL.S1–BL.S14 are reported in Figure 2.

is concave. The leaf margin is entire. The shape of the leaf apex is obtuse to slightly acute. The surface of leaves locally shows the outlines of epidermal cells, mainly near the margin. The adaxial cuticle of the leaves is slightly thicker than the abaxial cuticle; they are 3–11 μm and 3–7 μm thick, respectively. The leaves are amphistomatic. On the abaxial surface, the stomatal apparatuses are arranged in longitudinal rows that converge toward the leaf apex or are more or less randomly distributed (Fig. 8a–b). On the adaxial surface, they are more dispersed. The stomatal apparatuses of the

abaxial surface are slightly larger than those of the adaxial surface. They are 44–66 μm long and 32–46 μm wide, and 37–52 μm long and 27–41 μm wide, respectively (Fig. 8c–d). The stomatal rows are not sunken, but the guard cells of individual stomata are sunken in a pit. The pit apertures are circular to oval, measuring 6–16 μm in diameter. Their orientation is not consistent. The pit apertures are oriented obliquely, longitudinally or transversally relative to the leaf margin. The subsidiary cells form a thick and well-marked rim around the pit apertures. The guard cells are not visible from

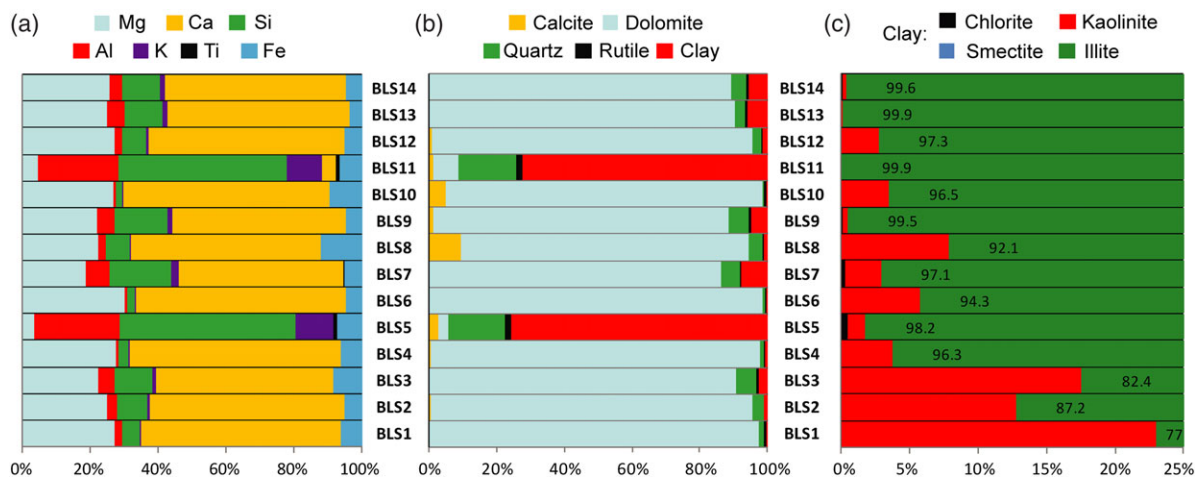


Fig. 5. (Colour online) Chemical, mineralogical and clay composition of the diverse levels from the Bleynard quarry. (a) Chemical composition obtained using XRF analyses. (b) Mineralogical composition obtained using XRD analyses. (c) Clay distribution in the <2 µm decarbonated fraction. The stratigraphic locations of samples BLS1–BLS14 are reported in Figure 2.

the external surface of the cuticle. The ordinary epidermal cells are square, rectangular or polygonal, and are 9–53 µm long and 7–31 µm wide. They form longitudinal rows that are oriented parallel to the leaf axis (Fig. 8e–f). The anticlinal walls of ordinary epidermal cells are straight and are up to 2–6 µm thick. The outer periclinal walls of the epidermal cells are more or less convex but do not form individual papillae.

Remarks. Although SEM micrographs provided information about the outer surface of the cuticle remains, their inner surface was commonly not well-preserved and therefore it was difficult to observe. The stomatal apparatuses were not well-preserved from the inner surface of the cuticle.

Pagiophyllum peregrinum (Lindley & Hutton) A. Schenk emend. Kendall and *Brachyphyllum paparelii* Saporta are the most common plant remains from the Hettangian–Sinemurian floras of the Causses Basin (Thévenard, 1992, 1993; Moreau *et al.* 2019b). However, although the gross morphology of *P. peregrinum* is highly variable (Thévenard & Barbacka, 1999), it shares many similarities with *B. paparelii* (Thévenard, 1993). As explained by Thévenard (1992), it is difficult to distinguish between both taxa when considering only the gross morphology of the leafy axes and leaves. The leaves of *P. peregrinum* can be as long as broad with a rounded apex, as well as longer than wide with an acute apex. *Brachyphyllum paparelii* and *P. peregrinum* can be almost exclusively distinguished by its cuticular features, mainly from stomatal apparatuses (Thévenard, 1993). Both show haplocheilic stomatal apparatuses with typical subsidiary cells displaying rim-shaped thickening. However, in *B. paparelii*, this rim-shaped thickening bears clearly individualized papillae in the top part. These papillae are not present in *P. peregrinum*. We may note that some species of *Brachyphyllum* such as *B. cyclophorum* Reymanovna from the Liassic of Poland, *B. ardenicum* T. M. Harris from the Middle Jurassic of Yorkshire (Harris, 1979), and *B. trautilii* Barale & Contini from the Middle Jurassic of France (Barale, 1981) also show an absence of papillae on stomatal apparatuses. *Brachyphyllum cyclophorum* differs from *P. peregrinum* in its irregular arrangement of the stomata (Thévenard, 1993). *Brachyphyllum ardenicum* mainly differs in that it has a thicker cuticle and by the absence of stomatal apparatuses on the adaxial surface of the leaves (Harris, 1979). *Brachyphyllum trautilii* differs in

that it shows scattered stomatal apparatuses that are never organized in longitudinal rows converging toward the leaf apex.

Pagiophyllum peregrinum was reported from several Hettangian–Sinemurian localities of France, with the most famous being from Ardennes, Aveyron, Hérault, Lozère and Vendée (Thévenard, 1992; Thévenard *et al.* 1995, 2003). The size of the leaves from Bleynard is slightly smaller than that of specimens commonly observed in the Causses Basin and Ardennes (Thévenard, 1992; Thévenard *et al.* 1995). We can note that *Pagiophyllum ?kurrii* from the Hettangian of Aveyron (southern France; Thévenard, 1992) and *P. araucarinum* (Pomel) Saporta from the Hettangian of Vendée (western France; Thévenard *et al.* 2003) differ from *P. peregrinum* in the presence of well-developed papillae on the stomatal apparatuses.

Male cones

Classostrobus sp. Alvin, Spicer & J. Watson

Material. M486_2020.4_1b; M486_2020.4_9 to M486_2020.4_12.

Description. The five cones are spherical to ovoid, 7.0–15.5 mm long and 8.0–11.5 mm wide and bear helically arranged microsporophylls (Fig. 9a–d). The length/width ratio of the cones is 1.5–1.7. The microsporophylls are flattened to convex, triangular in shape and are longer than they are wide. They show a large base and an acute apex. The abaxial surface is slightly keeled along the total length of the microsporophyll. The microsporophylls are up to 4.8 mm long and up to 2.5 mm wide. The microsporophyll margin is entire.

Remarks. SEM analyses reveal pollen grains along broken microsporophylls; however, it is not possible to determine the number and arrangement of the pollen sacs. The gross morphology and size of the grains (c. 20–25 µm) suggest an affinity with *Classopollis* sp. It can be noted that *Classostrobus* Alvin, Spicer & J. Watson species from several Jurassic localities yielded pollen grains ascribed to *Classopollis* H. D. Pflug or *Corollina* Malyavkina (Barale, 1987; Van Konijnenburg-Van Cittert, 1987; Thévenard, 1993).

In France, the male cone *Classostrobus* was rarely reported from the Hettangian–Sinemurian deposits (Barale, 1987; Thévenard, 1993). In the Causses Basin, only two Hettangian–Sinemurian localities yield specimens of the genus (Thévenard, 1992). Based on seven specimens from Chaldecoste (Mende), Thévenard

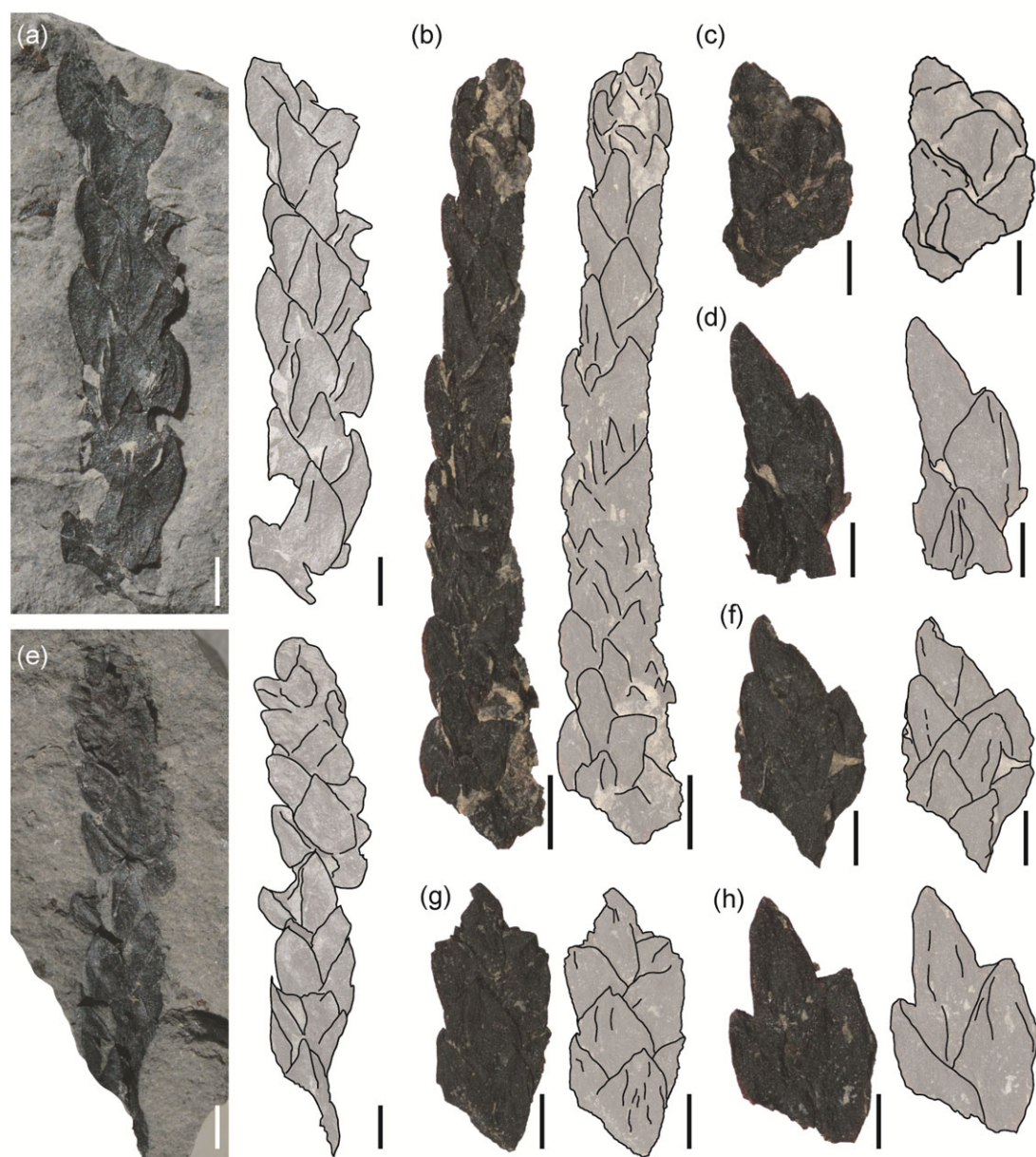


Fig. 6. (Colour online) Leafy axes of *Pagiophyllum peregrinum* from the Hettangian of Bleyard (level 7), stereomicroscopic images. (a–h) Narrow shoots showing persistent, helically arranged, highly appressed, imbricated and triangular to rhomboidal leaves. Specimens: (a) M486_2020.4_1a, (b) M486_2020.4_2, (c) M486_2020.4_3, (d) M486_2020.4_4, (e) M486_2020.4_8, (f) M486_2020.4_5, (g) M486_2020.4_6, (h) M486_2020.4_7. All scale bars = 2 mm.

(1993) proposed a new species, *C. lozerianus* Thévenard. Although *Classostrobus* specimens from Bleyard are clearly bigger than those from Chaldecoste (see Thévenard, 1993), male cones from the two localities show a similar gross morphology.

Wood

Brachyoxylon cf. *voisinii* Thévenard, Philippe & Barale
Material. M486_2020.4_18.

Description. The wood is a tracheidoxyl, with marked growth-rings and narrow late woods, limited to a few cell layers. No resin channels or axial parenchyma were observed. The tracheids often have a rounded cross-section, and their radial pits are found at the bottom of an oblique furrow (Fig. 10a), which suggests a compression wood. The tracheids are narrow, measuring roughly 10 µm in diameter. Tracheid pitting occurs on the radial wall only, with pits that are either round and spaced or contiguous and slightly

compressed (Fig. 10a). As estimated from the limited possible observations, the two types of radial pitting are equally frequent and distributed randomly through the growth-rings. Rays are 2 to 9 cells high (mean = 3.6; $n = 37$), homogeneous and slightly heterocellular. The marginal ray cells are broader than inner ray cells, but of variable width, and their outer limit draws a wavy line (Fig. 10b). Ray cells are short, usually crossing no more than three tracheids. Their walls are thin and unpitted, except for the cross-fields. These have two to six cupressoid oculipores disposed in an araucarioid way (Fig. 10c).

Remarks. Although we can confidently assign this specimen to *Brachyoxylon* Hollick & Jeffrey (Philippe & Bamford, 2008), the limited nature of the observations, in particular of the radial pitting of the tracheids, means that we are less sure of the species identifications; we feel it most likely belongs to *Brachyoxylon voisinii*

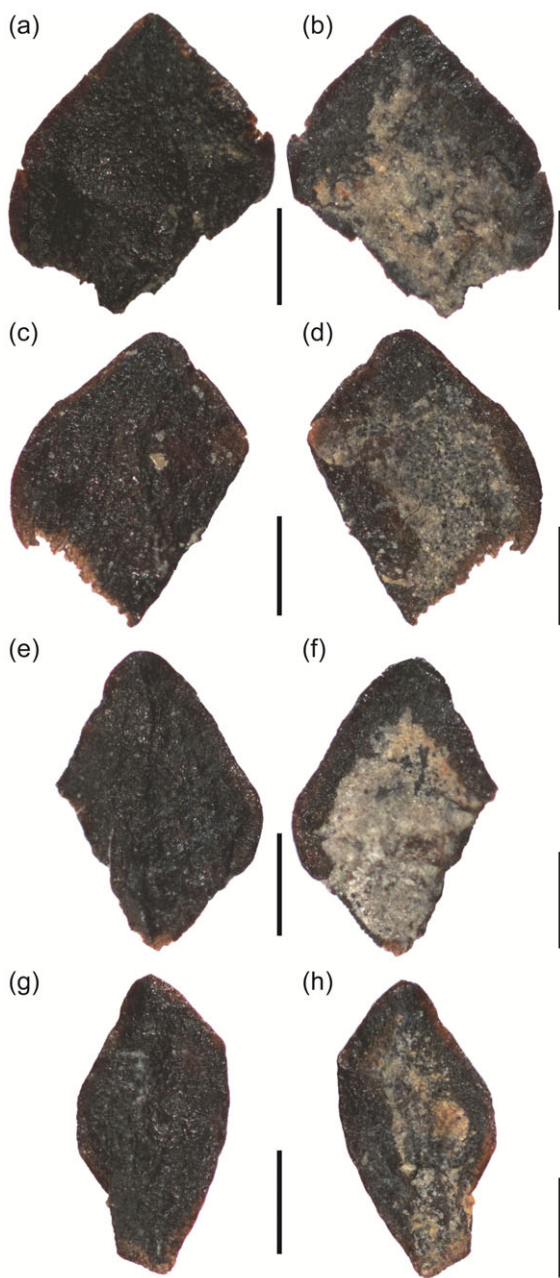


Fig. 7. (Colour online) Triangular to rhomboidal leaves of *Pagiophyllum peregrinum* from the Hettangian of Bleynard, stereomicroscopic images. The abaxial surface of the leaves (a, c, e, g) is convex, whereas the adaxial surface (b, d, f, h) is concave. Specimens: (a) M486_2020.4_13, (b) M486_2020.4_14, (c) M486_2020.4_15, (d) M486_2020.4_16. All scale bars = 1 mm.

Thévenard, Philippe & Barale, though this is not certain. *Brachyoxylon liebermannii* Philippe has a more abietinean radial pitting of the tracheids and more pits per cross-field, while *Brachyoxylon trautii* (Barale) Philippe has a more araucarian radial pitting of the tracheids, where the abietinean pits are almost limited to late wood, and also with more pits per cross-field (Philippe, 1995). A well-preserved and very similar material from a nearby locality, Mende, was identified as *B. voisinii* (Moreau *et al.* 2019b).

Pollen grains

Classopollis classoides Pflug
Material. M486_2020.4_19.

Description. The pollen grains are oblate or isodiametric, and oval to circular in polar and equatorial view (Fig. 9e–g). The polar axis is 20–25 µm long and the equatorial axis is 15–20 µm long. The proximal pole shows a tetrad mark. The exine is tectate with infratectal structures and an equatorial rimula (infratectal striate band). The equatorial band is 5–7 µm wide. The exine is 1–2 µm thick.

Remarks. The specimens ($n = 237$) were counted under a light microscope and are all ascribed to *Classopollis classoides* H. D. Pflug. Distal cryptopores are not observed. This pollen was previously described as *Corollina torosus* (Reissinger) Klaus in the Hettangian deposits from the Causses Basin (Thévenard, 1992, 1993). As explained in Jersey & McKellar (2013), ‘*Traverse* (2004) proposed conservation of the name *Classopollis* against *Corollina* and *Circulina*. This proposal, recommended by the Committee for Fossil Plants (Skog, 2005), was adopted by the International Botanical Congress, Vienna, 2005 (McNeill *et al.* 2006)’. *Traverse* (2004) stated: ‘*Couper* (1958) formally transferred *Pollenites torosus* to *Classopollis torosus*, and this is often cited as the correct name for *Classopollis classoides*. *Reissinger*’s (1950) *Pollenites torosus* was not validly published because it lacks a description or diagnosis, as required by the ICBN [International Code of Botanical Nomenclature]’. In this context we follow the suggestions of *Traverse* (2004) and *Jersey & McKellar* (2013), and prefer to use *Classopollis classoides* rather than *Corollina torosus*.

4.b.2. Dinosaur tracks

The observed tracks consist of three tridactyl footprints comprising traces of digits II, III and IV. They are weakly marked and consist of concave epireliefs. The footprints may obtain a score of 1 to 2 as per the morphological preservation scale of *Marchetti et al.* (2019). The dinosaur footprints are all isolated and no trackway was observed. Two morphotypes can be distinguished.

Morphotype 1

Description. The first morphotype consists of an isolated footprint (Bl_T1; Fig. 11a–b). The track is longer than wide ($L/W = 1.3$), 29.0 cm long and 21.5 cm wide. The divarication angle II–IV is 33°. Impressions of the digits are quite well-defined and elongated. The traces of digits III and II are the longest and the shortest imprints, respectively. The position of the digito-metatarsal pad of digit IV is more proximal than for digit II. There is no plantar impression.

Remarks. These tracks share similarities with *Grallator* Hitchcock from the Early Jurassic of the Causses Basin: they are longer than wide and have a long free part of digit III, a small divarication angle II–IV and slender digit impressions. In the Hettangian–Sinemurian deposits of the Causses Basin, four ichnospecies of *Grallator* were previously reported, *G. lescurei* Demathieu, *G. minusculus* Hitchcock, *G. saulierensis* Demathieu & Sciau, and *G. variabilis* de Lapparent & Montenat (Demathieu *et al.* 2002). The dimensions of the track included in Morphotype 1 are close to those of *G. lescurei* and *G. minusculus* ($L = 12.5–36.0$ cm and 24–35 cm, respectively; Demathieu *et al.* 2002). However, based on a single and poorly preserved footprint, this material cannot be conclusively ascribed to an ichnospecies.

Morphotype 2

Description. The second morphotype is represented by two isolated footprints (Bl_T2 and Bl_T3; Fig. 11c–d, e–f). The tracks are as long as they are wide ($L/W = 1.0–1.1$), 22.0 cm long and 15.5–22.0 cm wide. The divarication angle II–IV varies from 51° to 57°. The digit impressions are moderately elongated and show claw marks. On Bl_T2, the imprints of the pads are preserved and

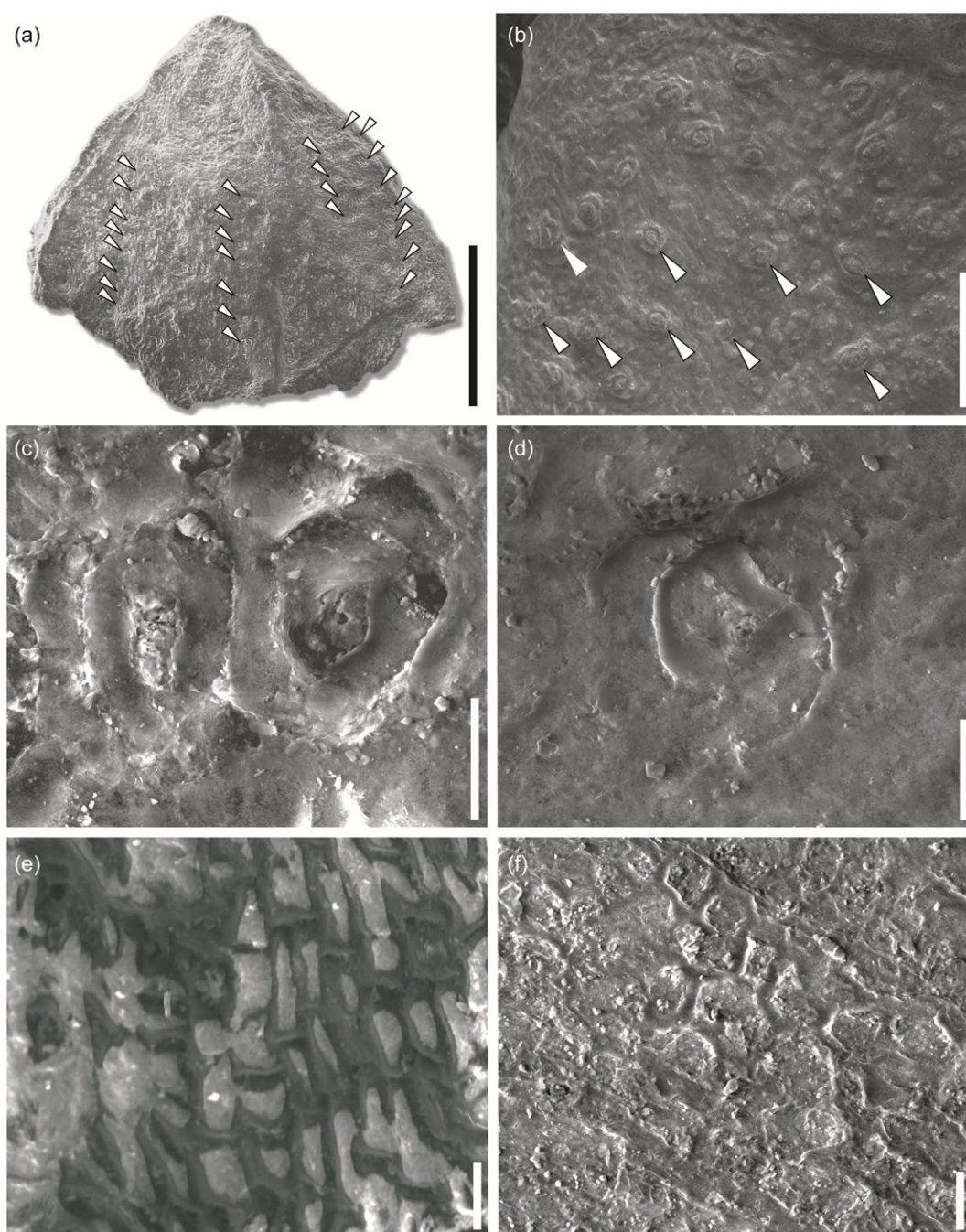


Fig. 8. *Pagiophyllum peregrinum*, SEM microphotographs of the leaf cuticles. (a–b) Abaxial view showing the alignment of the stomatal apparatuses. (c–d) Stomatal apparatuses with a thick and well-marked rim around the pit apertures, adaxial surface. (e) Outer surface of the cuticle showing longitudinal parallel rows of rectangular, polygonal to square ordinary epidermal cell outlines, adaxial view. (f) Inner surface of the cuticle showing polygonal to square ordinary epidermal cells, adaxial view. Specimen: M486_2020.4_17. Scale bars: (a) = 1 mm; (b) = 250 µm; (c–f) = 25 µm.

are circular to oval. The impression of the proximal plantar surface is marked on Bl_T2 (Fig. 11c–d).

Remarks. These tracks differ from Morphotype 1 because the footprints are as long as they are wide, and they show a larger divarication angle II–IV. These features are similar to those of tracks previously ascribed to *Dilophosauripus williamsi* Welles and which were reported from several Hettangian–Sinemurian tracksites in France (e.g., Demathieu & Sciau, 1992; Demathieu, 1993; Demathieu *et al.* 2002; Demathieu & Gand, 2003; Sciau, 2003; Gand *et al.* 2007; Moreau *et al.* 2014). *Dilophosauripus williamsi* was established based on tracks from the Early Jurassic of the United States of America (Welles, 1971). Given that the type material is poorly preserved, the validity of this ichnotaxon was strongly debated (Lockley & Hunt, 1995; Lucas *et al.* 2006;

Lockley *et al.* 2011; Gand *et al.* 2018). It is interesting to note that some authors consider *Dilophosauripus* as a junior synonym of *Eubrontes* Hitchcock (see references in Lucas *et al.* 2006; Lockley *et al.* 2011). Recently, based on morphometric similarities, Gand *et al.* (2018) recommended using *Kayentapus* rather than *Dilophosauripus* for the lowermost Jurassic tracks of the Causses Basin.

5. Discussion

5.a. Depositional palaeoenvironments

Carbonate platform sediments of the Hettangian Dolomitic Formation were deposited in the context of the earliest Jurassic

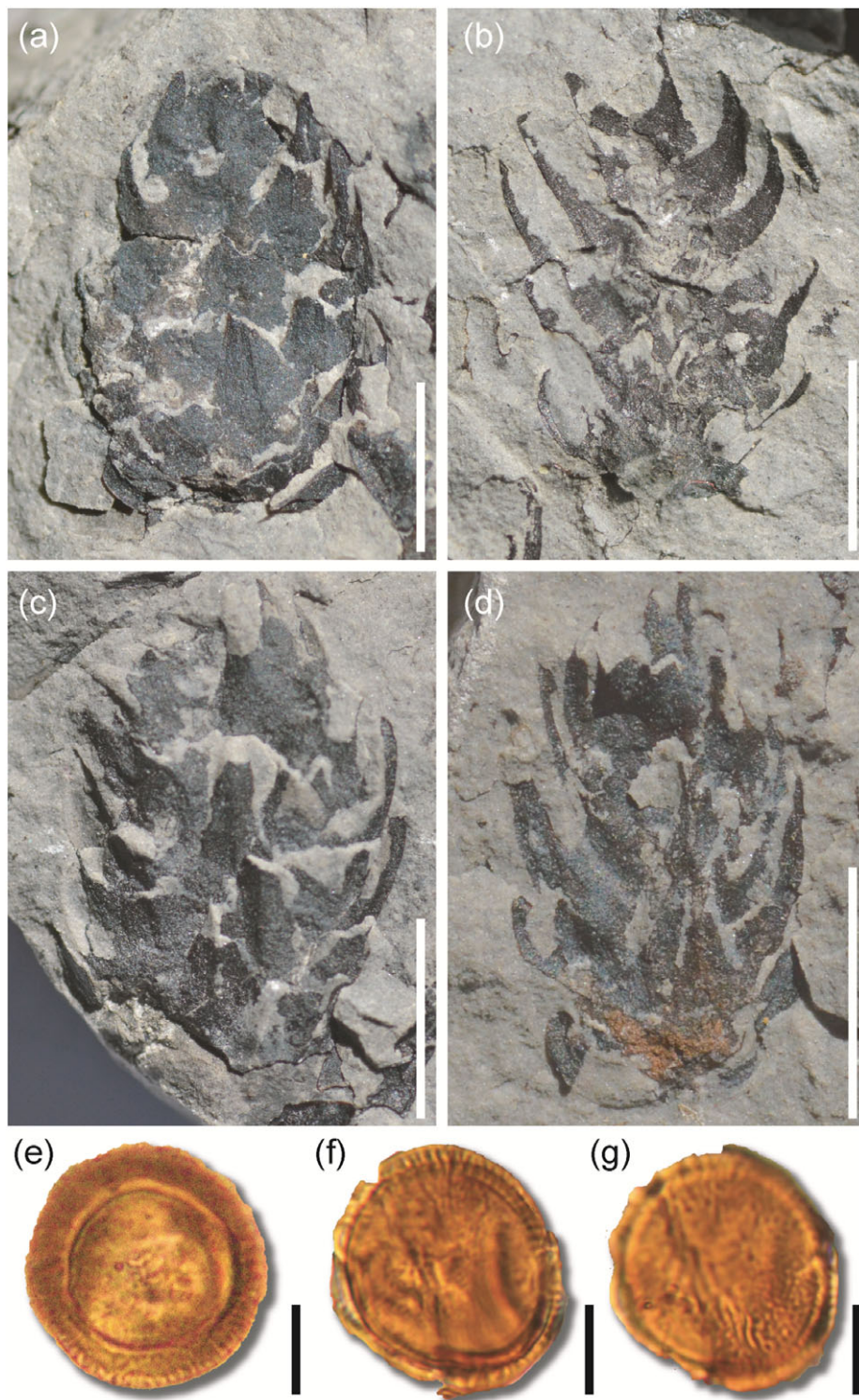


Fig. 9. (Colour online) *Classostrobus* sp., light microscope microphotographs. (a–d) Spherical to ovoid cones showing helically arranged microsporophylls; the microsporophylls are flattened to greatly convex, triangular in shape, longer than wide, and they show a large base and acuminate apex. (e–g) Pollen grains of *Classopollis classoides* in the proximal polar view (e), distal polar view (f) and equatorial view (g). Specimens: (a) M486_2020.4_9, (b) M486_2020.4_10, (c) M486_2020.4_11, (d) M486_2020.4_12. Scale bars: (a–d) = 0.5 cm; (e–g) = 10 μ m.

Tethyan marine transgression (Hamon, 2004). The lithological characteristics as well as the co-occurrence of marine and terrestrial organisms suggest that the sediments from the Bleyard quarry were deposited in a panel of marginal-littoral palaeoenvironments (Table 1). Based on field observations, together with microfacies and mineralogical analyses, we identified various depositional environments (Table 1).

At the base of the stratigraphic section, the sandy dolomite displaying megaripple marks with oblique stratifications and coquinas (F1) was deposited in shoreface environments regularly impacted by storm currents (Swift *et al.* 1983). Laterally, the local breccia lenses bearing limestone lithoclasts correspond to very proximal and high-energy foreshore domains (beach?). The alternation between dolomudstone organized in planar beds and

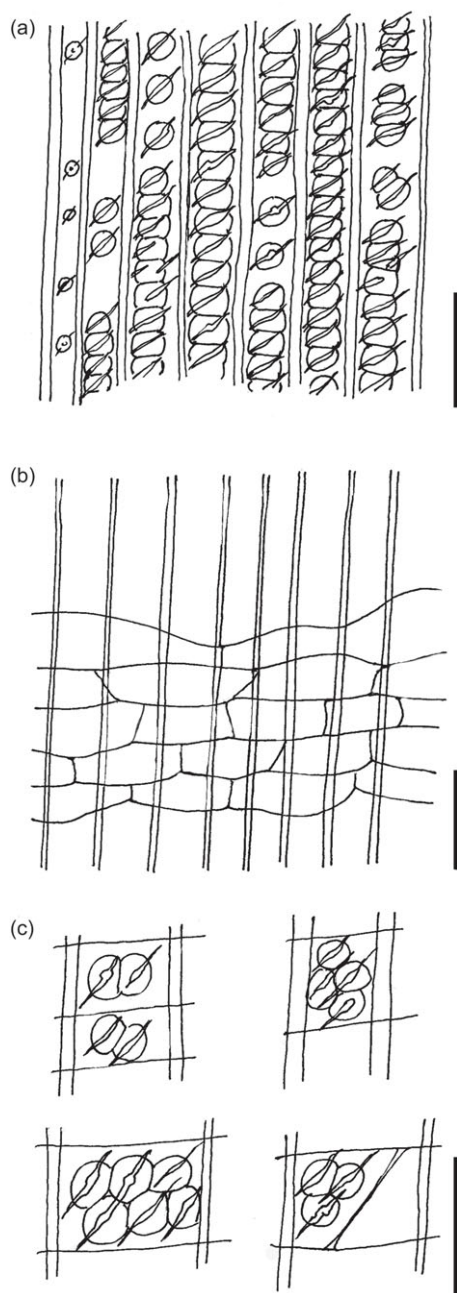


Fig. 10. Schematic illustrations of wood. (a) Radial view, pitting on the radial wall of the tracheids, from early wood (right) to late wood (left); all pit pores are open at the bottom of an oblique furrow, suggesting wood compression or alteration. (b) Radial view, cellular detail of a wood ray; note the short ray cells and the wavy margins. (c) Radial view, four non-contiguous cross-fields; note the araucarioid disposition of the oculipores and the cracks resulting from alteration. Scale bars: (a–b) = 50 μm; (c) = 25 μm.

yielding plants (F2) with lenses of lignitic clay (F3) marks the installation of lower-energy, restricted and shallow water environments. The abundance of leafy axes, cones, wood and pollen of conifers in level 7 (F4) indicates strong terrestrial inputs. The absence of marine organisms in the plant-bearing levels suggests that the environment was probably not open to the sea and that it was locally paralic. The preservation of long conifer twigs and the absence of morphological sorting indicate that when the plant debris was transported, it was not over a long period of time, over a

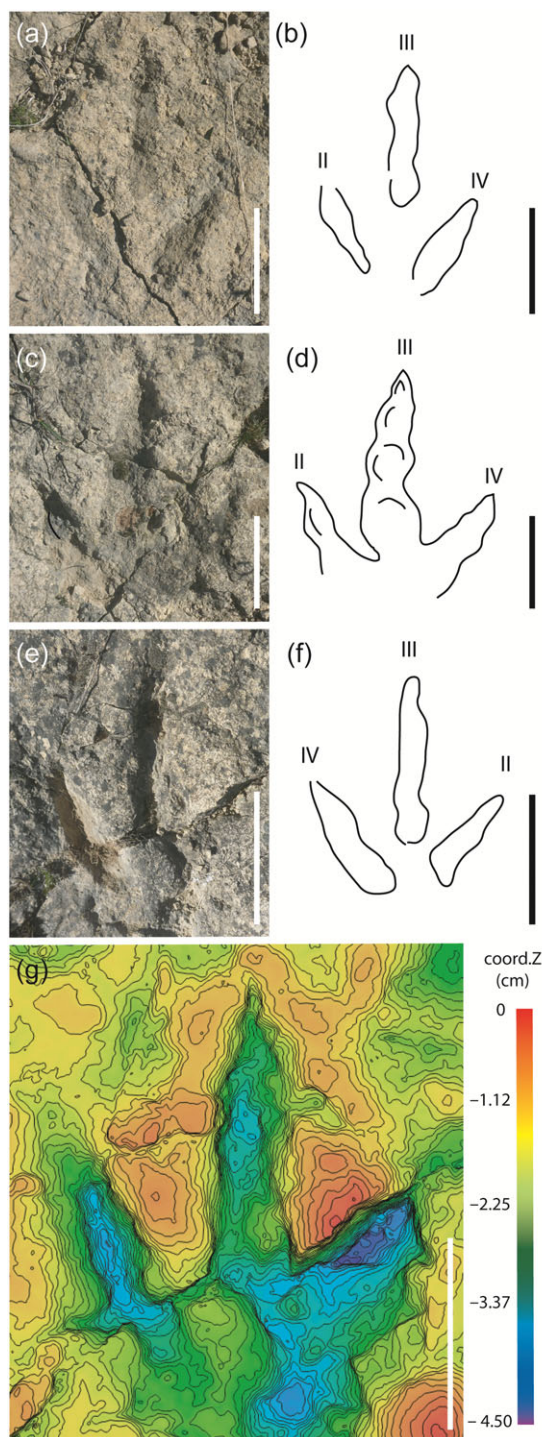


Fig. 11. (Colour online) Tridactyl dinosaur footprints from the Hettangian of the Bleybard quarry. (a–b) Morphotype 1: photograph (a) and interpretative sketch (b). (c–g) Morphotype 2: photographs (c, e), interpretative sketches (d, f) and digital elevation model (g). Specimens: (a–b) = BL_T1; (c–d) = BL_T2; (e–g) = BL_T3. All scale bars = 10 cm.

long distance or under low hydrodynamism. It suggests the parautochthony of the remains composing the taphocoenosis. In the upper part of the section, the cryptalgal laminites of the F5 facies are characteristic of regularly flooded intertidal and supratidal zones (e.g. Alsharhan & Kendall, 2003; Hamon, 2004; Matysik, 2016). The lack of bioclasts and coarse sediment suggests limited

storm-generated transport. All the elements of this facies may reflect a relative distance to the subtidal zone. At the top of the section, the surfaces bearing mud cracks, ripple-marks and dinosaur footprints indicate that sediments were deposited in environments with a thin layer of water which were periodically emerged (tidal flat). The absence of invertebrate skeletons suggests restricted life conditions, probably related to high salinity. At Mende, 25 km west of the Bleynard quarry, the Dolomitic Formation yielded halite pseudomorphs that attest to local evaporitic conditions (Moreau, 2011).

5.b. Origin and significance of clay minerals

Two types of clay assemblages are identified, either a mixture of illite and kaolinite in dolomitic facies or a clay fraction composed entirely of illite in marly layers (Fig. 5c). As shown by Daoudi & Deconinck (1994), the very good crystallinity of kaolinite in a porous dolomitic facies suggests an authigenic origin. In the Hettangian Dolomitic Formation from the Escalette section (50 km south of the Bleynard quarry; Marza *et al.* 1998), the pervasive authigenic development of kaolinite in the porosity of the dolomites has been observed by SEM (JF Deconinck, unpublished data). However, SEM observations of several samples from the Bleynard quarry did not show clay particles, probably because the total amount of clay mineral in these facies is too small. Therefore, our data cannot be used to definitively conclude the authigenic origin of the kaolinite, but this origin is highly suspected based on the XRD profiles. The unusual high-intensity ratio of the diffraction peaks of the quartz at 4.26 and 3.33 Å occurring in the clay fraction of the dolomitic facies (Figs 4–5; Fig. S1 and Tables S1–S3 in the Supplementary Material available online at <https://doi.org/10.1017/S001675682100039X>) suggests that the tiny quartz grains are authigenic in origin, which is common in evaporitic environments (Chen *et al.* 2016).

In the Mesozoic sediments, clay fractions composed of pure illite are very uncommon, since the erosion of continental areas leads to mixtures of minerals including chlorite, illite, smectite and kaolinite for the most encountered clay minerals. A monomineral clay fraction composed of pure illite is difficult to explain in terms of detrital inputs since illite usually indicates the deep erosion of crystalline rocks (Chamley, 1989). Such intense erosion is not consistent with the sedimentological context of the study area corresponding to a carbonate platform. Therefore, a detrital origin of illite can be discarded.

Similarly, pure, poorly crystallized illitic clay fractions were first described in Purbeckian sediments (Jurassic/Cretaceous transition) outcropping in the Jura Mountains (Deconinck & Strasser, 1987; Deconinck *et al.* 1988, 2001) where illitic minerals originated from the illitization of smectite at surface temperature in shallow supratidal environments subjected to wetting and drying cycles. This process was subsequently described in Cenozoic formations on the Isle of Wight (southern England; Huggett & Cuadros, 2005, 2010). The depositional environments of the Bleynard samples are quite similar to that described for the Purbeckian environments. Therefore, we suggest that the illite from the marly layers interstratified in the dolomitic succession have the same origin, i.e. an illitization of smectite at surface temperature in a carbonate platform environment submitted to repeated wetting (by seawater) and subsequent drying cycles. These conditions clearly indicate that a warm and probably seasonally humid climate prevailed during the Hettangian in southern France.

5.c. Implications for the dinosaur ecosystem and palaeoecophysiological insights

In the Causses Basin, theropod footprints were reported in several layers that correspond to deposits ranging from the Hettangian to the Sinemurian (Demathieu *et al.* 2002). However, bone remains of dinosaurs are still unknown in the Early Jurassic formations from this area. As shown by well-preserved tracks from the Dolomitic Formation (Demathieu *et al.* 2002), *Grallator* and *Kayentapus* are tridactyl footprints showing a similar phalangeal formula (type 3, 4 and 5 for toes II, III and IV). This deduced osteological architecture corresponds to that of theropod dinosaurs (Baird, 1957; Olsen *et al.* 1998; Demathieu *et al.* 2002). Body fossils of earliest Jurassic theropods were ascribed to Coelophysidea and Ceratosauria and reported in Africa, Antarctica, China and the USA (Weishampel *et al.* 2004; Smith *et al.* 2007; Xing *et al.* 2013). In Europe, rare theropod body fossils were reported in Hettangian deposits of England, France, Italy and Luxembourg (Larsonneur & Lapparent, 1966; Carrano & Sampson, 2004; Delsate & Ezcurra, 2014; Dal Sasso *et al.* 2018). In France, there is a unique occurrence of theropod bones in the Moon-Airel Formation (Normandie; Larsonneur & Lapparent, 1966). This material was ascribed to the Coelophysidae *Liliensternus airelensis* by Cuny & Galton (1993) and later assigned to *Lophostropheus airelensis* (Ezcurra & Cuny, 2007).

In Early Jurassic deposits from France, plant remains are rarely found associated with dinosaur footprints (Sciau, 1992). Similarly to the Veillon tracksite (in western France) which shows a co-occurrence of dinosaur tracks and abundant conifer cuticles (Lapparent & Montenat, 1967; Thévenard *et al.* 2003), the Bleynard outcrop is an opportunity to better understand the ecosystems in which dinosaurs roamed. Although plant remains are abundant in level 7, they are clearly weakly diversified as they are all related to Cheirolepidiaceae. Similarly, other studies have reported the co-occurrence of *Pagiophyllum*, *Classostrobus*, *Brachyoxylon* and *Classopollis* (Thévenard, 1993). It is tempting to hypothesize that twigs, cones, wood and pollen grains from Bleynard belong to the same conifer. However, since *Classopollis* is also known to co-occur with other cone and twig genera (e.g. *Frenelopsis*; Kvaček, 2000; see also discussion in Van Konijnenburg-Van Cittert, 1987) this hypothesis cannot be verified. In other Hettangian–Sinemurian floras from the Causses Basin, Barale *et al.* (1991) and Thévenard (1992) estimated that conifers constituted ~98 % of foliar remains (mainly *Pagiophyllum peregrinum* and *Brachyphyllum paparelii*) and Pteridospermales (*Thinnfeldia obtusa* A. Schenk and *Thinnfeldia rhomboidalis* Ettingsh.) made up the remaining ~2 %. In addition, rare Cycadales (*Ctenozamites* Nathorst emend. T. M. Harris), Filicales (*Clathropteris platyphylla* Brongn.) and Ginkgoales (*Eretmophyllum caussenense* Thévenard; see Saporta, 1873; Ressouche, 1910; Thévenard, 1992; Moreau *et al.* 2019b) were reported from other Hettangian–Sinemurian plant-yielding localities from the Causses Basin (e.g. Mende in Lozère). Similarly to data obtained from the Bleynard material, xylogenetic analyses ascribed wood from the Causses Basin to conifers alone (Thévenard, 1993; Moreau *et al.* 2019b).

Although the paucity of the plant assemblage contained in level 7 (Fig. 2) needs to be carefully interpreted, the taphonomy suggests that the taphocoenosis probably reflected the composition of the local flora. Garcia *et al.* (1998) stated that *Brachyoxylon*-dominated wood assemblages usually originate from nearby carbonate platforms. Such a poorly diversified conifer-dominated plant

assemblage is common in the Laurasian littoral floras during the Hettangian (e.g. Thévenard, 1992, 1993; Thévenard *et al.* 2003). From an ecophysiological point of view, some xerophytic characteristics of conifers such as *Brachyphyllum* and *Pagiophyllum* clearly show that the flora of the Causses Basin and the Bleyard Strait was adapted to withstand intense sunlight and coastal environments exposed to desiccant conditions coupled with salty sea spray, and dry conditions: fleshy shoots; adapted leaf morphology (short and small leaf pressed against the axis); thick cuticles; sunken stomata apparatuses with subsidiary cells forming a thick rim and sometime bearing papillae limiting the water loss; and narrow tracheids, even in the early wood. These features are those of a conifer-dominated flora in a tropical to subtropical climate with contrasted seasons cyclically dry (Thévenard *et al.* 2003; Karakitsios *et al.* 2015). Similar Hettangian *Pagiophyllum*-dominated floras were reported from several plant beds deposited in littoral context (western France; Thévenard *et al.* 2003). This suggests that the optimal habitat for *P. peregrinum* was a marginal-littoral environment that probably had strong marine inputs. In Europe, during the Jurassic, the wood genus *Brachyoxylon* had the southernmost distribution of a set of six wood genera (Philippe *et al.* 2017), and can probably be considered as indicative of a warm subtropical climate. *Brachyoxylon* was also hypothesized as characteristic of a tropophilous climate, with a marked alternation between a wet and a dry season (Oh *et al.* 2011). Here, palynology also supports this hypothesis, with *Classopollis* being mainly reported from sediments deposited in a littoral context and under a warm tropophilous climate (Srivastava, 1976; Vakhrameev, 1981, 1987).

Some lowermost Jurassic archosaur tracksites from the Causses Basin also yield rare trackways ascribed to *Batrachopus* and which attest to the presence of crocodylomorphs in a theropod-rich ecosystem (Demathieu & Sciau, 1992; Demathieu *et al.* 2002; Moreau *et al.* 2019a). Moreover, rare footprints from the Hettangian dolomite of Aveyron and Lozère were tentatively ascribed to ornithopods (Demathieu *et al.* 2002; Moreau, 2011). Considering the local presence of woodlands along the Hettangian–Sinemurian coasts, we could suppose that this vegetation was probably an attractive and important source of food for megaherbivorous dinosaurs. However, data collected from more than 60 Hettangian–Sinemurian tracksites of the Causses Basin (e.g. Demathieu *et al.* 2002; Moreau *et al.* 2014, 2018), as well as traces from the Bleyard Strait, suggest that lowermost Jurassic dinosaur communities from these areas were mainly composed of theropods. Since Hettangian sauropod tracks were abundantly reported in marginal-marine paralic facies from other areas of Laurasia (Gierliński *et al.* 2004), the absence of their trackways in the littoral environments of the Causses Basin and the Bleyard Strait raises questions.

6. Conclusions

- The quarry studied here constitutes the first dinosaur tracksite reported from the Bleyard Strait. It represents one of the rare Hettangian archosaur tracksites from France yielding plant-rich beds. The two morphotypes of tridactyl dinosaur tracks share similarities with *Grallator* and *Kayentapus*. The plant assemblage exclusively yields remains of Cheirolepidiaceae conifers (*Pagiophyllum peregrinum*, *Classostrobus* sp., *Brachyoxylon* sp., *Classopollis classoides*).

- Sedimentological, petrological and mineralogical analyses demonstrated that, in the Dolomitic Formation from Bleyard, the palaeoenvironment progressively evolved from shoreface/foreshore domain (facies F1) to a restricted shallow environment that was only partially/occasionally open to the sea (facies F2 to F4), then an intertidal to supratidal zone (tidal flat; facies F5).
- This study supports that theropods were abundant and particularly adapted to tidal flats that were periodically emerged and bordering paralic environments inhabited by littoral Cheirolepidiaceae-dominated forests.
- The xerophytic characteristics of the flora as well as the clay mineral analyses suggest tropical to subtropical climate with contrasting seasons, cyclically dry then humid.

Supplementary material. To view supplementary material for this article, please visit <https://doi.org/10.1017/S001675682100039X>

Acknowledgements. We would like to express our gratitude to the Society Llorens and particularly Guillaume Llorens who authorized the access to the quarry. We thank Lara Sciscio, Johanna HA van Konijnenburg-van Cittert and the anonymous reviewer for their constructive and thoughtful reviews of the manuscript. We thank Emilie Steimetz for her technical contribution during SEM investigations. This research did not receive any specific grants from any funding agencies, commercial or not-for-profit sectors.

Declaration of interest. The authors have no known conflict of interest.

References

- Alsharhan AS and Kendall CSC (2003) Holocene coastal carbonates and evaporites of the southern Arabian Gulf and their ancient analogues. *Earth-Science Reviews* **61**, 191–243.
- Baird D (1957) Triassic reptile footprint faunules from Milford, New Jersey. *Harvard College Museum of Comparative Zoology Bulletin* **117**, 449–520.
- Barale G (1981) La paléoflore jurassique du Jura français: étude systématique; aspects stratigraphiques et paléoécologiques. *Documents Laboratoire Géologie Faculté Lyon* **81**, 1–467.
- Barale G (1987) Les Cheirolepidiacées du Jurassique inférieur de Saint-Fromond, bassin de Carentan (Manche-France). *Bulletin de la Société Botanique de France, Actualités Botaniques* **134**, 19–37.
- Barale G, Philippe M and Thévenard F (1991) L'approche morphologique en paléobotanique: application à l'étude du Jurassique. *Geobios* **13**, 57–67.
- Biscaye PE (1964) Distinction between kaolinite and chlorite in recent sediments by x-ray diffraction. *American Mineralogist* **49**, 1281–9.
- Bish DL and Post JE (1993) Quantitative mineralogical analysis using the Rietveld full-pattern fitting method. *The American Mineralogist* **78**, 932–40.
- Briand B, Combémol R, Couturié J-P, Bérard P and Vaurrelle C (1993) *Notice explicative, carte géologique au 1/50.000 de la France, feuille du Bleyard (863)*. Orléans: Bureau de Recherches Géologiques et Minières, 76 pp.
- Briand BG, Couturié J-P, Geffroy J and Gèze B (1979) *Notice explicative, carte géologique au 1/50.000 de la France, feuille de Mende (862)*. Orléans: Bureau de Recherches Géologiques et Minières, 52 pp.
- Brouder P, Gèze B, Macquar JC and Paloc H (1977) *Notice explicative, carte géologique au 1/50.000 de la France, feuille de Meyrueis (910)*. Orléans: Bureau de Recherches Géologiques et Minières, 29 pp.
- Brusatte SL, Benton MJ, Ruta M and Lloyd GT (2008) The first 50 Myr of dinosaur evolution: macroevolutionary pattern and morphological disparity. *Biology Letters* **4**, 733–6.
- Carrano MT and Sampson SD (2004) A review of coelophysoids (Dinosauria: Theropoda) from the Early Jurassic of Europe, with comments on the late history of the Coelophysoidea. *Neues Jahrbuch für Geologie und Paläontologie Monatshefte* **9**, 537–58.
- Chamley H (1989) *Clay Sedimentology*. Berlin/Heidelberg: Springer, 623 pp.

- Chen X, Chafetz HS, Andreassen R and Lapen TJ (2016) Silicon isotope compositions of euhedral authigenic quartz crystals: implications for abiogenic fractionation at surface temperatures. *Chemical Geology* **423**, 61–73.
- Couper RA (1958) British Mesozoic microspores and pollen grains, a systematic and stratigraphic study. *Palaeontographica Abteilung B* **103**, 75–179.
- Cuny G and Galton PM (1993) Revision of the Airel theropod dinosaur from the Triassic–Jurassic boundary (Normandy, France). *Neues Jahrbuch für Geologie und Paläontologie, Abhandlungen* **187**, 261–88.
- Dal Sasso C, Maganuco S and Cau A (2018) The oldest ceratosaurian (Dinosauria: Theropoda), from the Lower Jurassic of Italy, sheds light on the evolution of the three-fingered hand of birds. *PeerJ* **6**, e5976.
- Daoudi L and Deconinck J-F (1994) Contrôles diagénétique et paléogéographique des successions sédimentaires argileuses du bassin atlasique au Crétacé (Haut-Atlas occidental, Maroc). *Journal of African Earth Science* **18**, 123–34.
- Deconinck J-F, Gillot P-Y, Steinberg M and Strasser A (2001) Syn-depositional, low temperature illite formation at the Jurassic–Cretaceous boundary (Purbeckian) in the Jura Mountains (Switzerland and France); K/Ar and delta¹⁸O evidence. *Bulletin de la Société Géologique de France* **172**, 343–8.
- Deconinck J-F and Strasser A (1987) Sedimentology, clay mineralogy and depositional environment of Purbeckian green marls (Swiss and French Jura). *Eclogae Geologicae Helvetiae* **80**, 753–72.
- Deconinck J-F, Strasser A and Debrabant P (1988) Formation of illitic minerals at surface temperatures in Purbeckian sediments (Lower Berriasian, Swiss and French Jura). *Clay Minerals* **23**, 91–103.
- Delsate D and Ezcurra MD (2014) The first Early Jurassic (late Hettangian) theropod dinosaur remains from the Grand Duchy of Luxembourg. *Geologica Belgica* **17**, 175–81.
- Demathieu G (1990) Problem in discrimination of tridactyl dinosaur footprints, exemplified by the Hettangian trackways, the Causses, France. *Ichnos* **1**, 97–110.
- Demathieu G (1993) Empreintes de pas de dinosaures dans les Causses (France). *Zubia* **5**, 229–52.
- Demathieu G and Gand G (2003) Les sites à traces de pas de vertébrés du Trias à l'Hettangien. Contenu et interprétation. *Le Naturaliste Vendéen* **3**, 47–53.
- Demathieu G, Gand G, Sciau J and Freyret P (2002) Les traces de pas de dinosaures et autres archosaures du Lias inférieur des Grands Causses, Sud de la France. *Palaeovertebrata* **31**, 1–143.
- Demathieu G and Sciau J (1992) Des pistes de dinosaures et de crocodiliens dans les dolomies de l'Hettangien du Causse du Larzac. *Comptes Rendus de l'Académie des Sciences de Paris* **315**, 1561–6.
- Demathieu G and Sciau J (1999) De grandes empreintes de pas de dinosaures dans l'Hettangien de Peyre (Aveyron, France). *Geobios* **32**, 609–16.
- Ellenberger P (1988) La découverte des pistes de dinosauriens de Camprieu. *Causses et Cévennes* **7**, 139–40.
- Ezcurra MD and Cuny G (2007) The coelophysoid *Lophostropheus airelensis*, gen. nov.: a review of the systematics of 'Liliensternus' *airelensis* from the Triassic–Jurassic outcrops of Normandy (France). *Journal of Vertebrate Paleontology* **27**, 73–86.
- Gand G, Demathieu C and Montenat C (2007) Les traces de pas d'amphibiens, de dinosaures et autres reptiles du Mésozoïque français: inventaire et interprétations. *Palaeovertebrata* **35**: 1–149.
- Gand G, Fara E, Durlot C, Caravaca G, Moreau J-D, Baret L, André D, Lefillatre R, Passet A, Wiénin M and Gély J-P (2018) Les pistes d'archosaures: *Kayentapus ubacensis* nov. isp. (théropodes) et crocodylomorphes du Bathonien des Grands-Causses (France). Conséquences paléo-biologiques, environnementales et géographiques. *Annales de Paléontologie* **104**, 183–216.
- García J-P, Philippe M and Gaumet F (1998) Fossil-wood in Middle–Upper Jurassic marine sedimentary cycles of France: relations with climate, sea-level dynamics, and carbonate-platform environments. *Palaeogeography, Palaeoclimatology, Palaeoecology* **141**, 199–214.
- Gèze B, Pellet J, Paloc H, Bambier A, Roux J and Senaud G (1980). *Notice explicative, carte géologique au 1/50.000 de la France, feuille de Florac* (886). Orléans: Bureau de Recherches Géologiques et Minières, 52 pp.
- Gierliński G, Pieńkowski G and Niedźwiedzki G (2004) Tetrapod track assemblage in the Hettangian of Sołtyków, Poland, and its paleoenvironmental background. *Ichnos* **11**, 195–213.
- Hamon Y (2004) *Morphologie, évolution latérale et signification géodynamique des discontinuités sédimentaires: exemple de la marge Ouest du Bassin du Sud-Est (France)*. Thesis, University of Montpellier II, Montpellier, France. Published thesis.
- Harris TM (1979) *The Yorkshire Jurassic flora. V. Coniferales*. London: Natural History Museum, 166 pp.
- Hillier S (2000) Accurate quantitative analysis of clay and other minerals in sandstones by XRD: comparison of a Rietveld and a reference intensity ratio (RIR) method and the importance of sample preparation. *Clay Minerals* **35**, 291–302.
- Hillier S (2003) Quantitative analysis of clay and other minerals in sandstones by X-Ray Powder Diffraction (XRPD). In *Clay Mineral Cements in Sandstones* (eds RH Worden and S Morad), pp. 213–51. International Association of Sedimentologists, Special Publication no. 34.
- Huggett JM and Cuadros J (2005) Low-temperature illitization of smectite in the late Eocene and early Oligocene of the Isle of Wight (Hampshire basin), U.K. *American Mineralogist* **90**, 1192–1202.
- Huggett JM and Cuadros J (2010) Glauconite formation in lacustrine/palaeosol sediments, Isle of Wight (Hampshire Basin), UK. *Clay Minerals* **45**, 35–49.
- Jersey NJ de and McKellar JL (2013) The palynology of the Triassic–Jurassic transition in southeastern Queensland, Australia, and correlation with New Zealand. *Palynology* **37**, 77–114.
- Karakitsios V, Kvaček Z and Mantzouka D (2015) The first plant megafossil in the Early Jurassic of Greece: *Brachyphyllum* (Coniferales) from the Lower Posidonia Beds (Toarcian) in the Ionian zone (NW Greece) and its palaeogeographic implications. *Neues Jahrbuch für Geologie und Paläontologie, Abhandlungen* **278**, 79–94.
- Klug HP and Alexander LE (1974) *X-Ray Diffraction Procedures: For Polycrystalline and Amorphous Materials*. New York: Wiley 992 pp.
- Kvaček J (2000) *Frenelopsis alata* and its microsporangiate and ovuliferous reproductive structures from the Cenomanian of Bohemia (Czech Republic, Central Europe). *Review of Palaeobotany and Palynology* **112**, 51–78.
- Lapparent AF (de) and Montenat C (1967) Les empreintes de pas de reptiles de l'Infralias du Veillon (Vendée). *Mémoires de la Société Géologique de France* **46**, 1–43.
- Larsonneur C and Lapparent AF (de) (1966) Un dinosaurien carnivore, *Halticosaurus*, dans le Rhétien d'Airel (Manche). *Bulletin de la Société Linnéenne de Normandie* **10**, 108–16.
- Leonardi G (1987) *Glossary and Manual of Tetrapod Footprint Palaeoichnology*. Brasília: Publicação do Departamento Nacional da Produção Mineral Brasil, 75 pp.
- Lockley MG and Hunt AP (1995) *Dinosaur Tracks and Other Fossil Footprints of the Western United States*. New York: Columbia University Press, 338 pp.
- Lockley MG, Gierliński G and Lucas SG (2011) *Kayentapus* revised: notes on the type material and the importance of this theropod footprint ichnogenus. *New Mexico Museum of Natural History and Science* **53**, 330–6.
- Lucas SG, Klein H, Lockley MG, Spielmann JA, Gierliński GD, Hunt AP and Tanner LH (2006) Triassic–Jurassic stratigraphic distribution of the theropod footprint ichnogenus *Eubrontes*. *New Mexico Museum of Natural History and Science Bulletin* **37**, 86–93.
- Malafosse (de) G (1873) Recherches sur le Lias de la région de Marvejols. *Bulletin de la Société d'Agriculture, Industrie, Sciences et Arts du Département de Lozère* **24**, 5–56.
- Marchetti L, Belvedere M, Voigt S, Klein H, Castanera D, Díaz-Martínez I, Marty D, Xing L, Feola S, Melchor RN and Farlow JO (2019) Defining the morphological quality of fossil footprints. Problems and principles of preservation in tetrapod ichnology with examples from the Palaeozoic to the present. *Earth-Science Reviews* **193**, 109–45.
- Marty D (2008) Sedimentology, taphonomy, and ichnology of Late Jurassic dinosaur tracks from the Jura carbonate platform (Chevenez-Combe Ronde tracksite, NW Switzerland): insights into the tidal-flat

- palaeoenvironment and dinosaur diversity, locomotion, and palaeoecology. *Geofocus* **21**, 1–278.
- Marza P, Séguret M and Moussine-Pouchkine A** (1998) Fischer plot and spectral analysis applied to cyclostratigraphy of Liassic carbonates of the southern 'Causse du Larzac', south France. *Bulletin de la Société Géologique de France* **169**, 547–62.
- Matysik M** (2016) Facies types and depositional environments of a morphologically diverse carbonate platform: a case study from the Muschelkalk (Middle Triassic) of Upper Silesia, southern Poland. *Annales Societatis Geologorum Poloniae* **86**, 119–64.
- McNeill J, Barrie FR, Burdet HM, Demoulin V, Hawksworth DL, Marhold K, Nicolson DH, Prado J, Silva PC, Skog JE, Wiersema JH and Turland NJ** (2006) International Code of Botanical Nomenclature (Vienna Code). *Regnum vegetabile* **146**, 1–260.
- Moore DM and Reynolds RC** (1997) *X-Ray Diffraction and the Identification and Analysis of Clay Minerals*. New York: Oxford University Press, 322 pp.
- Moreau J-D** (2011) *Nouvelles découvertes d'empreintes de dinosaures en Lozère. Analyse biométrique des traces et synthèse paléoenvironnementale de l'Hettangien*. Mende: Association Paléontologique des Hauts Plateaux du Languedoc, 34 pp.
- Moreau J-D, Baret L, Trincal V and André D** (2012a) Empreintes dinosauroïdes de l'Hettangien de Gatuzières (Lozère, France). In *Ichnologie dinosaurienne du Jurassique de Meyrueis*. Mende: Association Paléontologique des Hauts Plateaux du Languedoc, 5–11.
- Moreau J-D, Fara E, Néraudeau D and Gand G** (2019a) New Hettangian tracks from the Causses Basin (Lozère, southern France) complement the poor fossil record of earliest Jurassic crocodylomorph in Europe. *Historical Biology* **31**, 341–552.
- Moreau J-D, Gand G, Fara E and Michelin A** (2012b) Biometric and morphometric approaches on Lower Hettangian dinosaur footprints from the Rodez Strait (Aveyron, France). *Comptes Rendus Palevol* **11**, 231–9.
- Moreau J-D, Philippe M and Thévenard F** (2019b) Early Jurassic flora from the city of Mende (Lozère): synthesis of the historical sites, new sedimentological, palaeontological and palaeoenvironmental data. *Comptes Rendus Palevol* **18**, 159–77.
- Moreau J-D and Thévenard F** (2018) Rediscovery of the 'destroyed' holotype of *Weltrichia fabrei* Saporta from the Rhaetian/Hettangian of Lozère (Southern France). *Geodiversitas* **40**, 521–7.
- Moreau J-D, Trincal V, André D, Baret L, Jacquet A and Wienin M** (2018) Underground dinosaur tracksite inside a karst of southern France: Early Jurassic tridactyl traces from the Dolomitic Formation of the Malaval Cave (Lozère). *International Journal of Speleology* **47**, 29–42.
- Moreau J-D, Trincal V, Gand G, Néraudeau D, Bessière G and Bourel B** (2014) Two new dinosaur tracksites from the Hettangian Dolomitic Formation of Lozère, Languedoc-Roussillon, France. *Annales de Paléontologie* **100**, 361–9.
- Oh C, Legrand J, Kim K, Philippe M and Paik IS** (2011) Fossil wood diversity gradient and Far-East Asia palaeoclimatology during the Late Triassic – Cretaceous interval. *Journal of Asian Earth-Sciences* **40**, 710–21.
- Olsen PE, Smith JH and McDonald NG** (1998) Type material of the type species of the classic theropod footprint genera *Eubrontes*, *Anchisauripus* and *Grallator* (Early Jurassic, Hartford and Deerfield basins, Connecticut and Massachusetts, U.S.A.). *Journal of Vertebrate Paleontology* **18**, 586–601.
- Philippe M** 1995. Bois fossiles du Jurassique de Franche-Comté (nord-est de la France): systématique et biogéographie. *Palaeontographica Abteilung B* **236**, 45–103.
- Philippe M and Bamford M** (2008) A key to morphogenera used for Mesozoic conifer-like woods. *Review of Palaeobotany and Palynology* **148**, 184–207.
- Philippe M, Puijalón S, Suan G, Mousset S, Thévenard F and Mattioli E** (2017) The palaeolatitudinal distribution of fossil wood genera as a proxy for European Jurassic terrestrial climate. *Palaeogeography, Palaeoclimatology, Palaeoecology* **466**, 373–81.
- Reissinger A** (1950) Die 'Pollenanalyse' ausgedehnt auf alle Sedimentgesteine der geologischen Vergangenheit, II. *Palaeontographica Abteilung B* **90**, 97–126.
- Ressouche J** (1910) Horizon fluvio-lacustre au sommet de l'Hettangien en Lozère. *Bulletin de la Société d'étude des sciences naturelles de Béziers* **32**, 10–13.
- Rietveld HM** (1969) A profile refinement method for nuclear and magnetic structures. *Journal of Applied Crystallography* **2**, 65–71.
- Roquefort C** (1934) Contribution à l'étude de l'Infra-Lias et du Lias inférieur des Causses cévenols. *Bulletin de la Société Géologique de France* **5**, 573–94.
- Saporta (de) G** (1873) *Paléontologie française ou description des fossiles de la France, végétaux, plantes jurassiques*. Tome I, Algues, Equisetacées, Characées. Paris: Masson, 506 pp.
- Saporta (de) G** (1884) *Paléontologie française ou description des fossiles de la France, végétaux, plantes jurassiques*. Tome III, Conifères ou Aciculaires. Paris: Masson, 672 pp.
- Saporta (de) G** (1891) *Paléontologie française ou description des fossiles de la France, végétaux, plantes jurassiques*. Tome IV, types proangiospermes et supplément final. Paris: Masson, 558 pp.
- Sciau J** (1992) *Sur la piste des dinosaures des Causses*. Millau: Association des amis du Musée de Millau, 31 pp.
- Sciau J** (2003) *Dans les pas des dinosaures des Causses. Inventaire des sites à empreintes*. Millau: Association des Amis du Musée de Millau, 107 pp.
- Simon-Coinçon R** (1989) *Le rôle des paléoaérations et des paléoflores dans les socles: l'exemple du Rouergue (Massif Central Français)*. Thesis, Ecole des Mines de Paris, Paris, France. Published thesis.
- Skog JE** (2005) Report of the Committee for Fossil Plants: 6. *Taxon* **54**, 827.
- Smith ND, Makovicky PJ, Hammer WR and Currie PJ** (2007) Osteology of *Cryolophosaurus eliotti* (Dinosauria: Theropoda) from the Early Jurassic of Antarctica and implications for early theropod evolution. *Zoological Journal of the Linnean Society* **151**, 377–421.
- Snyder RL and Bish DL** (1989) Quantitative analysis. *Reviews in Mineralogy and Geochemistry* **20**, 101–44.
- Srivastava SK** (1976) The fossil pollen genus *Classopollis*. *Lethaia* **9**, 437–57.
- Swift DJ, Figueiredo AG, Freeland GL and Oertel GF** (1983) Hummocky cross-stratification and megaripples; a geological double standard? *Journal of Sedimentary Research* **53**, 1295–1317.
- Taylor JC and Hinczak I** (2006) *Rietveld Made Easy: A Practical Guide to the Understanding of the Method and Successful Phase Quantifications*. Canberra: Sietronics Pty Ltd, 201 pp.
- Thévenard F** (1992) *La paléoflore du Jurassique inférieur du bassin des Causses (France). Étude systématique, stratigraphique et paléo-écologique*. Thesis, Université Claude-Bernard, Lyon, France. Published thesis.
- Thévenard F** (1993) Les conifères du Jurassique inférieur du gisement de Chaldecoste, bassin des Causses (Lozère, France). *Review of Palaeobotany and Palynology* **78**, 145–66.
- Thévenard F and Barbacka M** (1999) Two leaf morphotypes of the *Pagiophyllum peregrinum* (Lindley et Hutton) Schenk emend Kendall from the Mecsek Mountains, Hungary. *Acta Palaeobotanica* **2**, 219–31.
- Thévenard F, Deschamps S, Guignard G and Gomez B** (2003) Les plantes fossiles du gisement hettangien de Talmont-Saint-Hilaire (Vendée, France). *Le Naturaliste vendéen* **3**, 69–87.
- Thévenard F, Philippe M and Barale G** (1995) Le delta hettangien de La Grandville (Ardennes, France): étude paléobotanique et paléoécologique. *Geobios* **28**, 145–62.
- Thiry M, Carrillo N, Franke C and Martineau N** (2013) *Technique de préparation des minéraux argileux en vue de l'analyse par diffraction des Rayons X et introduction à l'interprétation des diagrammes*. Fontainebleau: Centre de Géosciences, Ecole des Mines de Paris, 34 pp.
- Traverse A** (2004) Proposal to conserve the fossil pollen morphogeneric name *Classopollis* against *Corollina* and *Circulina*. *Taxon* **53**, 847–8.
- Trincal V, Charpentier D, Buatier MD, Grobety B, Lacroix B, Labaume P and Sizun J-P** (2014) Quantification of mass transfers and mineralogical transformations in a thrust fault (Monte Perdido thrust unit, southern Pyrenees, Spain). *Marine and Petroleum Geology* **55**, 160–75.
- Trincal V, Thiéry V, Mamindy-Pajany Y and Hillier S** (2018) Use of hydraulic binders for reducing sulphate leaching: application to gypsiferous soil sampled in Ile-de-France region (France). *Environmental Science and Pollution Research* **25**, 22977–97.

- Vakhrameev VA** (1981) Pollen *Classopolis*: indicator of Jurassic and Cretaceous climates. *The Palaeobotanist* **28–29**, 301–7.
- Vakhrameev VA** (1987) Climates and the distribution of some gymnosperms in Asia during the Jurassic and Cretaceous. *Review of Palaeobotany and Palynology* **51**, 205–12.
- Van Konijnenburg-Van Cittert JH** (1987) New data on *Pagiophyllum maculosum* Kendall and its male cone from the Jurassic of North Yorkshire. *Review of Palaeobotany and Palynology* **51**, 95–105.
- Weishampel DB, Dodson P and Osmolska H** (2004) *The Dinosauria*. Berkeley: University of California Press, 862 pp.
- Welles SP** (1971) Dinosaur footprints from the Kayenta Formation of northern Arizona. *Plateau* **44**, 27–38.
- Xing L, Bell PR, Rothschild BM, Ran H, Zhang J, Dong Z, Zhang W and Currie PJ** (2013) Tooth loss and alveolar remodeling in *Sinosaurus triassicus* (Dinosauria: Theropoda) from the Lower Jurassic strata of the Lufeng Basin, China. *Chinese Science Bulletin* **58**, 1931–5.